2020

An Innovative Approach to Intraoperative Quality Assurance for Low Dose Rate Brachytherapy

Masoud Jalayer

An Innovative Approach to Intraoperative Quality Assurance for Low Dose Rate Brachytherapy

Masoud Jalayer

Supervisor:
Marco Petasecca

This thesis is presented as part of the requirement for the conferral of the degree:
Master of Science (Medical Radiation Physics)

This research has been conducted with the support of the Australian Government Research Training Program Scholarship

University of Wollongong
School of Physics

May of 2020

Abstract

BrachyView is a novel in-body imaging system, aimed to accurately localise brachytherapy sources using high-resolution pixelated silicon detectors and a pinhole collimator. In the recent years, many research projects have studied the different possibilities for real-time, intra-operative, dynamic dose treatment planning to increase the quality of brachytherapy implants. The capabilities of this pinhole camera were tested through a proof of concept study using four active seeds. A more clinically realistic scenario, using twenty active seeds implanted in a PMMA phantom, was the clear next step. To further imitate a clinical scenario, 20 seeds were implanted and imaged using a single pinhole lead collimator with a diameter of 400 μm. BrachyView was successful at locating the seeds within 1-2 mm of their expected positions which was verified via co-registration with a full clinical post-implant CT scan with 0.8 mm width.

The first BrachyView prototype to feature a triple-chip detector embedded within a tungsten collimator with three single cone pinholes was used to localise 30 active seeds embedded within 11 needles, implanted in a soft gel prostate phantom, under ultrasound guidance. For verification, a full post implant CT was also performed. The BrachyView was able to accurately resolve the all the seeds with a maximum discrepancy of 1.78 mm

Table of contents

Chapter One: Introduction

Brachytherapy is one of the most common modes of treatment of early stage prostate cancer. This treatment involves the implantation of a predetermined number of radioactive seeds (which is determined by the treatment type) within the prostate gland. Accurate localisation of the seeds within the prostate is key to estimating the dose received by the prostate and the surrounding tissue. This is an integral part of a successful treatment. The current methods for seed localisation suffer from low accuracy and high cost and cannot be performed in real time.

The BrachyView is a novel online seed localisation detector based on a high-resolution gamma camera which will assist in the Quality Assurance of Prostate Brachytherapy seed implantation.

In this study, the prototype detector is tested using live Low Dose Rate Brachytherapy seeds within a Polymethyl Methacrylate (PMMA) phantom, and a soft gel prostate phantom. Optimising the accuracy of seed localisation is the key objective of the experiments.

Chapter Two: Literature Review – Prostate Cancer and available Treatments

Prostate Cancer

In developed countries, the most diagnosed cancer among men is prostate cancer, this translates to the third most common cause death. It is believed that a positive family history, age and ethnicity are the strongest risk factors. There are several treatment methods available for localised and advanced prostate cancers, ranging from active surveillance to prostectomy to hormonal-deprivation treatments.
In the recent decades, there has been a substantial increase in prostate cancer diagnosis and this can be linked to better biopsy collection practices, the use of Prostate Specific Antigen (PSA) and public education.

Prostate tumours are most commonly diagnosed prior to metastasis, this increases chances of successful treatment as there is of range of treatment modalities available for localised prostate cancer, such as Prostectomy, radiation therapy or a combination of the two.
Active monitoring is also a very viable solution, as many diagnosed patients die with prostate cancer and not from it. This is because many cases of moderate to highly differentiated prostate cancers have a very indolent course, even when left untreated. Treatment methods of clinically localised prostate cancer depend on tumour characteristics and the patient's life expectancy.

Prostate cancer demonstrates little to no symptoms at its early stages. However, as it progresses, it can lead to urinary discomfort and presence of blood in the urine, Haematuria. Some of these symptoms are also common to other conditions prevalent in older men and are non-specific to prostate cancer. As prostate cancer progresses, it can also advance to the bones resulting in pain. [1]

The prostate is walnut-sized gland, measuring being 3-5 cm between its anterior and posterior borders. It is responsible for the production of a major constituent of seminal fluid, which is stored within tubular glands in the prostate. Prostate cancer originates within the cells of the glands, referred to as adenocarcinoma.
The main two prostate cancer screening methods are the PSA blood test and the Digital Rectal Examination (DRE). Elevated blood PSA levels can indicate prostate cancer however it is not a definite diagnosis. Prostatic hyperplasia, a non-malignant condition can also increase PSA levels in the blood. The PSA blood test is proven to be more sensitive than the DRE; however, the use of the two tests in conjunction is most effective as they are complementary. The PSA blood test has definitely increased the number of patients diagnosed with prostate cancer, this has led to over-diagnosis. This term refers to diagnosis of disease that would not necessarily affect the patients' life span or quality of life. Over-diagnosis can cause a negative financial cost and unnecessary pain and suffering for the diagnosed patients as a result of treatment. This has increased the detection of early stage prostate cancers; however, screening has not lead to a decreased regional cancer incidence.
This suggests that, contrary to common belief, screening has not reduced prostate cancer mortality, only increased the burden of low risk cancers.

If a PSA test and a DRE are both indicative of prostate cancer, the protocol examination is typically a core-needle biopsy of the prostate with either digital or ultrasound used as guidance. The acceptable standard is 12 biopsy samples (6 per prostate lobes), to be examined for cancerous cells. If cancer is present, a grade is assigned to the tumour based on the Gleason tumour grading system. This is done by assigning a score from 1 to 5 to the 2 most common tumour patterns identified, and the addition of these scores determines the Gleason grade. A higher score suggests more chance of metastasis. [2]

Treatment of Prostate Cancer

There are different modes of treatment available depending on the Gleason grade of the tumour, its advancement and size. Following diagnosis, the patient undergoes active surveillance. This involves further PSA and DRE examinations, and in some cases further biopsy samples.

Hormonal therapy or Androgen deprivation therapy refers to surgical or chemical castration in conjunction with Anti-Androgen medication. Another treatment method is Cryoablation which involves the freezing and thawing the prostate probes using gases under the guidance of Transrectal Ultrasound (TRUS).

There are different methods of External Bream Radiotherapy (EBRT) available for treatment of prostate cancer such as Intensity Modulated Radiation Therapy (IMRT), Conformal Radiation Therapy and Proton Radiation Therapy. High Intensity Focused Ultrasound Therapy utilises focused ultrasound to raise the temperature of the target cells and destroy them, and is also an option for prostate cancer patients.

Surgery is also an alternative treatment, ranging from removal of the entire prostate, seminal vesicles, ampulla of Vas Deferens and in some cases lymph nodes as well. The operation can be done by open or laparoscopic surgery. [2]

High dosage radiation treatment is generally the standard mode of treatment for patients diagnosed with intermediate and high risk locally advanced prostate cancer. Hormonal therapy can be used in conjunction with radiotherapy. This treatment modality has proved to offer long term control and high overall survival rates. Peeters et al. found that it is possible to further increase local tumour control by escalating the prescribed dose to 78 Gy or more. However, they also demonstrated that this treatment method tends to increase late genitourinary and gastrointestinal toxicity. [3]

IMRT offers the same treatment benefits, while avoiding the some of the adverse effects of the of radiotherapy. Zelefsky et al. reported that only 2% of patients treated with 81 Gy of IMRT experienced late grade 2 or higher gastrointestinal toxicity, compared with 14% of patients treated with the same dose, using three-dimensional radiotherapy. Despite the benefits of IMRT, this treatment method is not available in every centre. Dose escalation can also be achieved by adding a boost, typically delivered by a High Dose Rate Brachytherapy (HDR-BT). Better results and reduced toxicity levels can be achieved using HDR-BT. As this treatment method has a relatively sharp radiation level fall off, clinicians are able to deliver a higher biologically-equivalent dose to the tumour, while sparing the rectum and bladder. [4]

Brachytherapy

Brachytherapy is another type of therapy for localised prostate cancer and is also one of the most commonly utilised modes of treatment. The Latin word "Brachy" meaning near, distinguishes Brachytherapy from External Radiation Therapy. The radioactive agents are inserted directly into the tumour with the aim to maximise the delivered dose to the target tumour and minimise irradiation to the surrounding organs. Brachytherapy was one of the first types of radiotherapy used to treat cancer over a century ago. In its early days it was only used for treatment of superficial and easily accessible tumours. Prostate brachytherapy was first practiced by Willet Whitmore in the 1970s, however it proved to be a failure, despite its early success. The disappointing results were due a lack radiographic guidance during the source implants and no dose delivery plan. Also, due to late diagnosis, the prostate tumours treated were large and palpable, making them very unlikely to be treated using local treatments. During the 1980s, megavoltage external beam therapy with its clean, sophisticated and convenient procedure, coupled with an advanced planning system, became the more popular treatment method for localised prostate cancer. In the 1990s, prostate brachytherapy gained popularity among physicians due to several reasons. The first was the advent of the powerful screening method using PSA, allowing for early detection. The Second was developments of the TRUS which allowed for a more accurate seed placement method and patient convenience. There was a widespread disenchantment with the more common treatment methods such as surgical prostatectomy and External Beam Radiotherapy (EBRT), in the acceptance of brachytherapy as a standard therapy for prostate cancer. [5]

There are two main types of prostate Brachytherapy:

- High Dose Rate Brachytherapy

The less commonly used method, utilises High Dose Rate (HDR) seeds to deliver fractionated brachytherapy treatment. A HDR after-loader is used to temporarily place the seeds within the prostate for a prescribed amount of time. The insertion of these closed-ended needles is very similar to Permanent implants, and catheters replace the needles. These allow for the radioactive seeds to be passed through into the prostate. The after-loader is attached to the catheters via transfer tubes. The radiation source is removed from the patient after the delivery of the prescribed dose to the tumour.

- Low Dose Rate Brachytherapy

This treatment involves implanting permanent radioactive sources within the prostate using long hollow needles. During the procedure the patient is always placed in the dorsal lithotomy position, and the needles are inserted in the prostate using a standard grid. The seeds are placed within the hollow needles in front of a prod, and as the needles are retracted the seeds are deposited in the prostate. A typical treatment plan consists of more than 100 seeds. Many different radiopharmaceuticals and seed designs can be used in Low Dose Rate (LDR) Brachytherapy. Conventionally, Iodine 125 and Palladium 103 were used in LDR seeds. Also sources containing Cesium 131 were introduced in 2004. The treatment plan will typically include the seed type, this will depend on the physician and hospital preference.

Permanent Brachytherapy seeds are cylindrical and measure approximately 4.5mm in length and have a diameter around 0.8mm. The finer details of seeds' external shape, internal

structure and casing material vary with different seed models and manufacturers. The dose distribution will also be unique to the seed model and isotope used, and is affected by the internal structure, the thickness and type of cladding material. The of the most important characteristics of the seeds are the half-life and the energy of the photons emitted, and these are independent of the physical shape of the seeds. The most commonly used isotope in LDR Brachytherapy seeds is Iodine 125, with an ideal half-life of around 60 days and average photon emission energy equal to 27 keV. Another commonly used isotope is Palladium 103, with a much lower half-life of around 17 days with an average photon emission energy of 23 keV. Cesium 131 has a half-life of 9.7 days and average energy of 29 keV. The half-life of the isotope determines the speed with which the dose is deposited in the prostate, hence the importance of this characteristic. Using idone 125, 90% of the dose will be delivered in 197 days compared to 56 days when using seeds containing palladium 103.

TRUS-guided LDR Brachytherapy is the standard method of treatment for low- to moderate-risk locally advanced tumours. This treatment method has disadvantages such as possible seed migration, permanent radioactive implants in the prostate and its inability to deliver a high Biologically Equivalent Dose (BED) over a short period of time. HDR Brachytherapy avoids some of issues related to implanted seeds by utilizing a remote after-loading system (RALS). This system automatically deploys and retracts a single source of Iridium-192. The radioactive source is guided through the hollow implant needles, the sources are halted at specific positions in the patient (the dwell positions) for specific stop times (the dwell times). Additionally, the source is always contained within the implant needles, thus there is no risk of seed migration. There is also minimal exposure risk for the clinicians as there is no need for needle preparation. Inverse dose optimization planning allows for better theoretical dose distribution.

The HDR Brachytherapy has some significant benefits over LDR Brachytherapy as mentioned, however it also poses a potential for errors. Intra-operative patient movement, between the CT and treatment rooms can cause displacement of the implanted HDR catheters. As HDR Brachytherapy uses very high energy sources (Iradium-192: 380 KeV), a small internal displacement in seed position, will lead to large dosimetric variations. The high energy sources of HDR Brachytherapy, when compared to lower energy sources used for LDR Brachytherapy (Iodine-125 or Paladium-103), do not have a sharp dose fall-off. This can result in unnecessary and excessive irradiation of the vital surrounding organs. The catheters used in HDR Brachytherapy can also displace the gold marker fiducials for EBRT, which will lead to further dosimetric uncertainty. High Dose Rate Brachytherapy requires patient sedation and catheterization for each fraction delivered, this increases patient hospitalization time, cost and inconvenience. However, with Low Dose Rate therapy, the permanent radioactive implants may induce anxiety in the patient and family members, although the radiation the patient receives is negligible. [6]

As there exists no clinical trials directly comparing the effectiveness of available treatment methods, treatment choice ultimately depends on patient and physician preference. At present a number of different treatment methods are commonly used to successfully treat prostate cancer. Despite the success, each treatment modalities have its unwanted side effects and complications. The ultimate goal of treatment is to effectively eliminate the

existing cancerous tumour, thus preventing death or disability from prostate cancer, while simultaneously limiting treatment-related complications.
EBRT coupled with a single hypo-fractionated boost of 9 Gy HDR-BT is advantageous when compared to treatment schedules using multi-fractionated boosts. In multiple fractionated treatment regimes, there exists the risk of inter-fraction movement of marker seeds which are used for EBRT localisation. However, with the single fraction radiation delivery, errors due to needle displacement are avoided. Needle displacement can cause geometric variability, and to verify the needle depth a new CT may be needed. In a single fraction treatment spinal anaesthesia will only be used once. This will eliminate the trauma caused by multiple operations and reduces the overall impact on the patient's life. In terms of patient comfort, convenience and overall cost, single implant boost is advantageous, as it shortens hospitalization time, reduces the need for analgesia and minimizes the associated risk of deep venous thrombosis. [2]

Prostatectomy has been the most popular treatment type for prostate cancer in recent years. However, this procedure remains a challenging urologic surgery, due to the anatomical position of the prostate gland. The rectum, the bladder and the nerves supplying the penis are all within a close vicinity of the prostate, therefore an adequate resection aimed at total cancer control, could lead to loss of functions such as continence and potency. As a result of accurate screening procedures, the number of diagnosed cases of low-risk prostate cancer has increased significantly. The early detection means that the diagnosed patients are able to live for longer with prostate cancer and therefore places added emphasis on post-treatment quality of life. [7]

Radiobiology

With respect to radiobiology, the number of cancer cells destructed is proportional to the radiation dose delivered to the patient, unfortunately the same is true for the healthy surrounding tissue. The α/β ratio is an estimate of how radiation affects the various parts of the body, and is an excellent measure for comparing treatment plans concerning dose and number of fractions. The term, α, refers to the cells that will dies after a single hit of radiation, defining the initial slopr of the radiation dose-response curve. Conversely the term β describes the latter part of this slope and is related to the cells in the tumour that require more than one hit of radiation due to the ability to repopulate and repair. The α/β ratio estimates how sensitive cells are to the radiation, thus determining the effectiveness of the treatment. A high ratio suggests that target cells are rapidly multiplying, thus implying that low-dose radiation delivered over many fractions is more effective at destroying the cells. Conversely a low α/β ratio is characteristic of slowly proliferating cells, meaning high-dose radiation delivered in a few fractions will be more successful at cell destruction. The α/β ratio is used in the calculation of the BED.

$$BED = nd\left[1 + \frac{d}{\alpha/\beta}\right]$$

Where, *n* refers to the number of fractions and *d* is the dose delivered during each fraction. A low α/β ratio for the prostate tumour has been hypothesized (~ 1.5 Gy) suggesting that its cancerous cells are more susceptible to higher doses delivered in fewer fractions. Higher dose per fraction delivered to tumours with a lower α/β ratio than their surrounding healthy tissue, will result in a higher BED for the tumour than its surrounding healthy tissue, this would then increase the therapeutic ratio. [8]

Comparison of treatment Methods

Surgery and radiation therapy, whether it be in the form of EBRT or Permanent Prostate Brachytherapy (PPB) tend to have similar outcomes when treating patients with an early stage diagnosed disease. As expected, younger patients are equally concerned with the cancer survival outcome and quality of life after treatment, when choosing treatment type. As a result of this, post-treatment quality of life has gained increasing significance over the recent years.

The three main aspects concerning post-treatment quality of life are sexual, urinary and bowl function. Voulgaris et al. reports that, patients with PPB have significantly better post-treatment sexual function than those with high-dose EBRT or radical prostectomy. In addition, they approximate that 84% of the potent men treated at their centre, retain potency after treatment. In terms of urinary system dysfunction, the results are not as clear.

Following Brachytherapy, incontinence is very rare as suggested by the results gathered at the Guilford Cancer Centre. [8]

Bladder dysfunction is more common after brachytherapy treatment, and urinary incontinence is more prevalent post prostectomy. Urinary and sexual dysfunction are generally more common post radical surgery when compared to radiation treatment (EBRT, PPB or a combination of the two). However, issues concerning bowl function are more consistently reported by men who undergo radiotherapy than surgery. It is worthy to mention that most statistics concerning post-treatment quality of life, do not distinguish between Brachytherapy coupled with EBRT from mono-therapeutic Brachytherapy.

A quantitative evaluation of quality of life is very difficult to obtain, due to the significant bias placed on the matter by different individuals, also clinical and statistical data need to be considered. Nevertheless, if the patient prioritises potency and continence regarding quality of life post procedure Iodine 125 PPB implant may be the optimal form of definitive treatment. [9]

Brachytherapy Planning Procedures

Depending on the institution, the brachytherapy implantation procedure differs in treatment pre-planning, intra-operative planning and equipment. There are four main methods of implementation in regard to treatment planning:

- Preplanning: The treatment plan is prepared days or even weeks prior to the procedure using ultrasound and other imaging techniques (such as CT or MR imaging). The implantation is performed according to the treatment plan. It is crucial that the patient's anatomy is duplicated exactly from the volume study. Historically, this

planning system has the most amount of clinical experience and can produce great outcomes if performed correctly.

- Intra-operative: The ultrasound images and the volume study are used to construct treatment plan in the operating room. This method offers the great advantage of a more accurate patient geometry and volumetric study. However, some clinicians argue that this planning technique is flawed, as the pressures of preparing a complex treatment plan, while the patient is under anaesthetic and a large group of staff member waiting in the operating room, encourages mistakes, and discourages a thorough review of the treatment plan with an extended discussion of the treatment plan and consideration of the alternatives.

- Interactive: Using a pre-prepared as well as an intra-operative treatment plan, the operation is undertaken guided by ultrasound images. This technique offers some flexibility, as the treatment plan is altered according to the positioning of needles and the patient's anatomy deformation.

- Dynamic dose calculation is often adopted in this technique: Using ultrasound images of the prostate and the effective needle positions, the dose distribution is updated in real time. This allows for alteration of seed positions based on real time dose distribution and for a much more flexible procedure, and allows the physician to alter the plan to accommodate for under-dosed and over-dosed areas. This technique can increase time in the operating room, as the dose distribution has to be acquired after implanting the needles. Quality Assurance (QA) methods which accurately localise the seeds within the prostate in real time, from which the dose distributions can be recalculated are strongly desirable.

Quality Assurance and planning for brachytherapy

Quality Assurance for LDR brachytherapy is typically provided in real time, using a specialised ultrasound unit. The TRUS probe can acquire images axially or sagittally using two sets of separate ultrasound crystals. Both sets of images are helpful, in providing information about the positions of the needles in reference to anatomical features, i.e. prostate base and apex, rectum wall and urethra. The position of the TRUS probe is accurately adjusted by turning a knob connected to a "stepper" unit, which holds the probe securely in place. Each click of the stepper moves the TRUS probe crystals and the ultrasound image of 5 mm (standard clinical setting). The needle template is also mounted on the stepper unit, but it is fixed in respect to the patient and the TRUS longitudinal axis (see Figure 2.1). The standard template is a 13 by 13 grid of holes sized for needles. The rows are labelled from 0 to 6.5 in increments of 0.5 (5mm) from bottom to the top. The columns are designated by letters A, a, B, b etc. The grid pattern is also overlaid on the patient ultrasound image which is then co-registered with the grid on the stepper allowing for accurate insertion of the needles. [10]

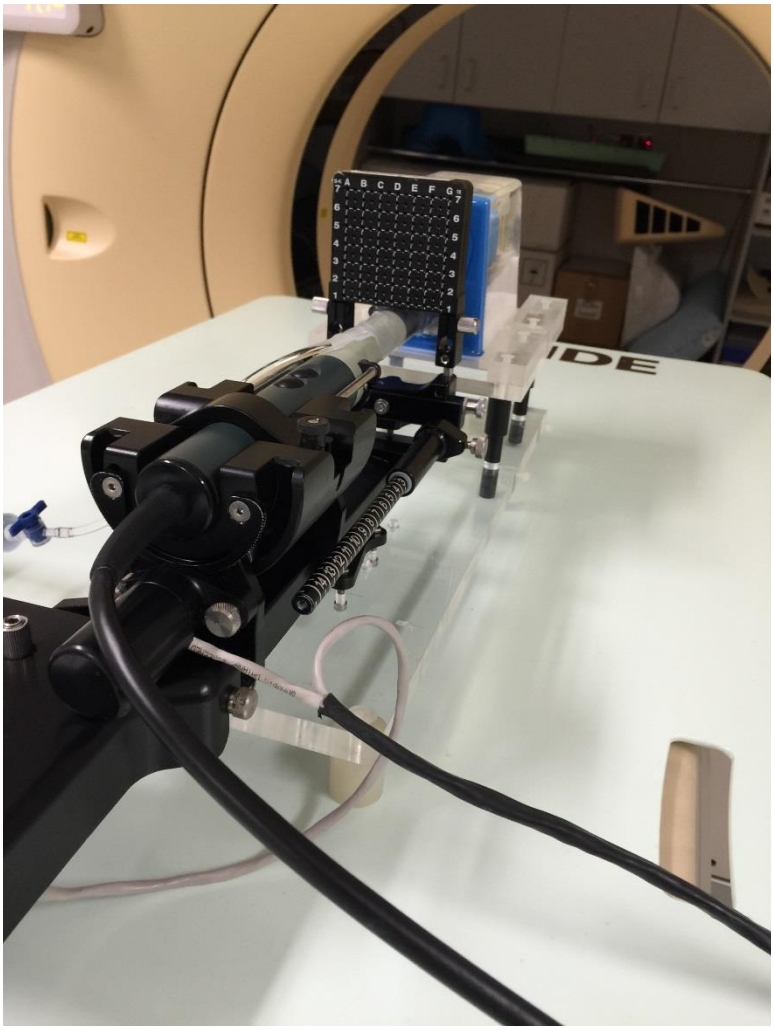

Fig.2.1: image of a TRUS probe setup on a plastic phantom; the grid template and the stepper unit are clearly visible. Taken by the author at the St. George Hospital.

To ensure that the pubic bone does not interfere with the needles, the patient is always situated in the dorsal lithotomy position. This position allows better access to the prostate and is easily reproducible when switching from the volume study to the implant operation. Prior to the operation it is essential to match the patient's anatomy from the volume study, to avoid discrepancies in the seeds' positions from the treatment plan.

Implant quality assurance in PPB is determined post-implant and can range from hours to weeks after the procedure. Computed Tomography (CT) imaging is recommended modality for post implant seed localisation. Variations in CT-obtained prostate volume can result in incorrect Dose Volume Statistics and Quality Assurance of the implantation. An excellent alternative to CT-based post implant examination is the TRUS, which is reproducible and is also used for intraoperative implantation guidance in PPB. There are some advantages and disadvantages using TRUS as a post implant dosimetry method. Automated seed sorting using CT is effective at seed localisation but is generally regarded as less effective to TRUS in determination of the prostate outline and volume determination. Also, CT seems to have a higher inter-observer variability in prostate segmentation than TRUS. This variability can result in differences in clinically relevant dosimetry parameters.

A dosimetry system based on TRUS is the more attractive to physicians as it is fast and low cost and is also more accurate in determining the prostate volume than CT-based systems. However, TRUS has a limited ability to localise seeds within the prostate, this is due to the reduced ultrasound back-scatter from standard seeds. There are ultrasound opaque seeds available on the market which are designed to be visible on a standard ultrasound dataset but they are expensive and rarely used clinically.
Transrectal Ultrasound is an excellent imaging tool used for the initial planning dosimetry for permanent prostate Brachytherapy. For post-implant dosimetry CT is most commonly used, for its superior imaging abilities especially for resolving high density seeds. Post-implant dosimetry is subject to a number uncertainties and difficulties, as the implantation can result in swelling and distortion of the prostate. Despite these challenges, an immediate (day 0) post-implant check can be very beneficial, as it presents the opportunity to intervene and re-implant in case of a large deviance from the treatment plan. A typical post-implant dosimetry is undertaken 4-6 weeks after the procedure, which allows operative effects to subside. The most significant uncertainties in post-operative dose calculations are caused by inter-observer variability. This is due to individual variability in contouring of the prostate volume. [11]

Due to the inherent but differing disadvantages of these methods, fusing the two modalities could potentially capitalize on the strengths of each modality. This could result in a more accurate and reproducible post-implant dosimetry procedure. This image fusion in real time will allow for immediate dosimetry, which will give the physicians the chance to correct any suboptimal implant in the operating room. [12]

In the study conducted by Daanen et al, the MR is brought to the operating room and combined with a TRUS probe, using a TRUS/MRI fusion technique. This does not require the presence of both the patient and the implantation team in the MRI room while assisting the clinician in treatment planning. This project reviews a rigid and an elastic co-registration of MRI and TRUS images. A pre-operative MRI of the prostate is acquired, three orthogonal T2 TSE volumes are obtained via an endo-rectal coil and the prostate contours are segmented jointly on the three volumes. Conventional axial TRUS slices are collected to produce a three-dimensional prostate model, intra-operatively. Ultimately the objective of the registration is a perfect superimposition of the prostate volumes. This process can also determine prostate movement and deformation pre- and intra-operatively. The co-registration is initialized by superimposing the centres of gravity of the two prostate volumes. This initial rough estimation can determine the rotation and translation parameters between datasets, and highlights any local deformations or distortions.
In this project, the initialization method uses an adaptive, hierarchical and regularized free-form deformation of the one volume to the other coordinate system. The optimization stage is based on the Levenberg-Marquadt minimization procedure. This produces a three-dimensional function, transforming any US data point to the corresponding MRI point. [13]

In a study conducted by Shaikh et al. the treatment plan is produced using a MRI-generated, contoured volume. The tumour contouring is done by an experienced physician and is reviewed by at least another experienced practitioner. The treatment is monitored by real time transrectal ultrasound. Rigid cystoscopy (the examination of the lining of the bladder and urethra) is performed by the oncologist to ensure the absence of needles and seeds in

the urethra or the bladder. Approximately four hours post-implant, the catheters are removed and the patient undergoes a post implant CT and MRI, to determine baseline dosimetry, this will be regarded as day-0. The patient will return for a day-21 dosimetric examination, via the same imaging techniques.
In this study the primary dose constraint was >145 Gy prescribed to 90% of the prostate volume (D90 > 145 Gy); a secondary constraint was that the volume of the prostate wuold receive >90% of the prescription dose (V100 >90%). Image fusion of CT and MRI are used for post implant dosimetry for day-0 and day-21, the contouring of the prostate is performed by the same physician to minimize variability. Comparison of the two post-implant dosimetric examinations allows physicians to check for seed position stability and quality assurance of the entire procedure, ensuring the prescribed dose is delivered to the tumour volume. As under-dosing the target area can lead to failed treatment. [14]

Another study under-taken by Takiar et al. investigates the advantages of using fused CT/MRI scans in conjunction with sector analysis for post-implant dosimetric analysis.
Takiar el al. uses sector analysis in place of dose-volume histograms to verify post-implant dosimetry. Sector analysis is a useful analytical tool that allows evaluation of the dose distribution to individual portions of the prostate in addition to the entire gland. This approach in post-implant dosimetry of the prostate, offers a significant advantage over standard dose-volume histogram analysis. As most patients treated with brachytherapy, are diagnosed with locally confined disease rather than involvement of the entire organ. Recognizing routinely under-dosed and over-dosed portion of the prostate will allow for improvement of treatment planning and delivery. The standardization of the sector analysis allows for comparison between patients and institutions, and also allows for findings to be evaluated in terms of outcomes and toxicity. It is admitted that the most significant limitation of sector analysis is that the quality of the output depends on the accuracy of the contouring. It is difficult to delineate the prostate apex and base on CT images, therefore many studies have suggested the fusion of CT and MR images as means of overcoming this limitation.
In this study, all patients selected were implanted with Palladium-103 stranded seeds according to the treatment plan designed under TRUS guidance. As a means of QA in the operating room, an anterior–posterior fluoroscopic image was acquired immediately after source implantation to grossly confirm placement as planned. CT images were then obtained using a 2.5 mm slice width to verify the quality of the implants. Another CT was performed on day 30; these images were used for the CT-based post-implant dosimetry to account for any prostatic edema due to the procedure.
All patients also underwent MR scans with 5 mm width on day 30. These images were then manually co-registered with the day 30 CT images using a point-based fusion. This method aligns selected seeds at the base and apex on the CT scan with the seed or needle-path voids on the MR image. Bony landmarks were not used to co-register the images due to the possibility of prostate movement as result of patient position and extent of bladder and rectum filling.
This clinical study has severe limitations, one of which was the follow up time. The mean follow-up time was 24 months; this is short by any means in comparison to other studies of similar objectives. Another potential factor for problems is the quality of co-registration of the two images. Imprecise fusion could negatively affect sector analysis and influence consequent interpretations.

Takiar el al conclude that their findings demonstrate the feasibility of CT/MRI- based post-implant dosimetry using sector analysis. This approach helped the team to accurately delineate the anatomical margins of the organ using the MR images. While sector analysis proved useful when comparing patients' treatment plans and outcomes. [15]

From the reviewed studies, it can be concluded that, **there are no available techniques for intra-operative quality assurance that is able to reconstruct the position of the seeds in Low Dose Brachytherapy or track the trajectory of the seeds in High Dose treatment**. The existing methods involve the use of an external source of radiation for imaging, which increases the total dose received by the patient, as well as treatment time and cost. The availability of real time tracking also allows the practitioners to alter the treatment plan to avoid under/over dosing critical target areas, if necessary. No feasible real-time techniques which are cost effective and do not use external radiation sources, have been proposed.

Chapter Three: BrachyView Concept

Centre of Medical Radiation Physics (CMRP) at University of Wollongong (Australia) proposes the BrachyView Project for both HDR and LDR treatments. This study will focus on the proof of concept BrachyView for Low Dose Rate Brachytherapy, using a large number of seeds in a plastic phantom and TRUS co-registration in a deformable gel phantom.

This research project proposes a novel in-body imaging technique using a high spatial resolution gamma camera embedded in a TRUS probe for real-time in vivo seed identification concurrent with a prostate ultrasound dataset. This tracking device consists of a planar pixelated silicon detector encased in a multi-pinhole tungsten collimator. The detector is aimed to have an accuracy of 1.5 mm with a sub-second temporal resolution.
The BrachyView probe consists of three side-by-side Medipix2 detectors. These detectors allow for a total imaging area of 14 x 42mm^2 (256 × 768 pixels with individual pixel size of 55 × 55μm^2), and were manufactured in collaboration with the Institute of Experimental and Applied Physics of Czech Technical University of Prague. The images of the radioactive seeds are acquired through the pinholes above the detector surface. In contrast to most pinhole systems, BrachyView works in demagnification mode (magnification factor of less than 1) which is made possible by the superior spatial resolution of the Medipix2 detectors. In Medipix2, each pixel has its own independent pre-amplification channel, coupled with two discriminator levels. This allows for the detection of each individual photon that strikes a pixel, where it will deposit its energy, and if this is higher than the energy threshold, increment the counter by one count. The count is then digitally readout by a USB interface with a refresh rate of a few hundred Hertz.

The presence of the tungsten collimator represents a potential problem for the rectum wall which could be affected by the dose enhancement generated by the backscattered radiation from the collimator.
A study by Han et al. set out to investigate the effects of such backscatter radiation. The experiments are accompanied by Monte Carlo simulations for confirmation purposes.
All experiments and simulations performed are aimed to measure Backscatter Dose Correction Factor, (BSDF), which is defined "as the ratio of the dose measured within a homogenous tissue equivalent volume with and without the presence of a high electron density region" [14] (i.e. tungsten collimator).
The simulations show that the backscattered electrons resulted in significant dose enhancement within very close proximity of the collimator. This is translated from a high value of BSDF, however this ratio rapidly diminished to unity (i.e. no measurable backscatter resulting in dose increase) at a distance less than 1 mm from the high Z material. The experimental results closely resembled the simulations for a planar tungsten collimator.
The team at CMRP then concluded, based on the measurements from the MOSkin and the results from the Monte Carlo simulations, that dose enhancement by backscattered electrons is expected to be negligible beyond 1mm from the collimator surface. The researchers also mention that the final probe will be encased in a protective 1 mm thick medical-grade

sterilisable tissue equivalent plastic shell, which will absorb the majority of the backscatter dose. [17]

As previously mentioned, following the treatment planned is crucial to the effectiveness of the procedure, as this ensures the tumour and surrounding tissue receive the prescribed dose. Therefore, localisation is vital to confirm that the treatment planned is followed as closely as possible. Intra-operative dynamic treatment planning allows for compensation of misplaced seeds, thus covering the cold spot they introduce. Intra-operative monitoring is imperative to maximize the benefits of prostate brachytherapy yet keeping the dose constraints to critical organs in check.
In a feasibility study of BrachyView for LDR brachytherapy, Petasecca et al. aim to reconstruct the spatial coordinates of four strategically placed seeds within a PMMA block mimicking the clinical brachytherapy grid positions. The placement of the four seeds, will effectively test out the gamma camera in the following ways:

- Evaluate the effect of the source to collimator distance (SCD)
- Evaluate the projected image quality of the two seeds positioned simultaneously, (one close to the camera and hence bright, and the other far producing a weaker signal)
- Verify the extension of the field of view (FOV) with implanted seed in the periphery.

The two most important parameters characterized in this work are the transverse and longitudinal resolution of the camera. The team at CMRP found that the transverse spatial resolution is in the submillimeter range, at low SCD. However, at a SCD of 60mm the transverse spatial resolution is 4mm, which is not acceptable for resolving brachytherapy seeds. A solution proposed, is to use a smaller pinhole with a diameter of 150-180 µm. A pinhole of this size will allow sufficient counts to be received by the detector while sparing the transverse spatial resolution at higher SCD. In contrast the longitudinal resolution is much more robust, and was found to only be affected by the focal length ($\propto 1/f^{20}$). This physical feature of the system must be very accurately determined.
The sensitivity of the spatial resolution of the camera highlights the significance of accurate manufacturing of the pinhole.

The focus of this project is the possibility to co-register the 3D coordinates obtained by the pinhole camera with the anatomical image of the prostate obtained by the TRUS prob. Due to its small size, this gamma camera can be integrated with a TRUS probe with dimensions of 22-24mm, which is acceptable for patient use. The integration of the two systems in one probe seems challenging from an engineering perspective, however the co-registration of the images will be relatively simple. The instrument will have an ultrasound transceiver and the triple chip Medipix2 detector along with its pinhole collimator on opposite halves of the cylindrical probe. Sharing the same central plane will allow for an easy co-registration algorithm, as they would also share a common spatial coordinate frame. The cylindrical shell will be ultrasound and radiation transparent, and will be in contact with the rectal wall. The inside apparatus can be rotated on a central axis, allowing easy transition between the two imaging systems. [18]

The BrachyView rectal probe design is based on a multi-pinhole lead collimator and three side by side Medipix2 detectors. Each element of the probe is presented below, beginning with a description of Medipix, a study for the optimisation of the tungsten collimator and the description of the technique used to reconstruct the position of the gamma source in 3D using triangulation. Figure 3.1 is a schematic representation of the BrachyView probe concept.

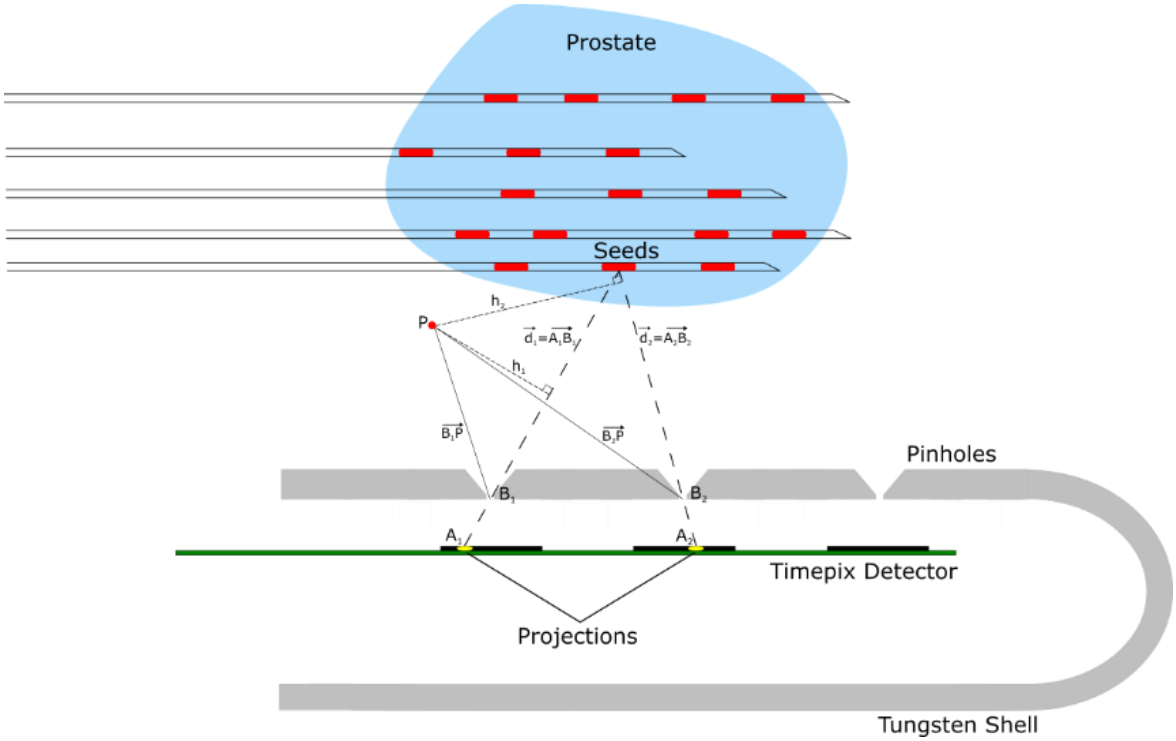

Fig.3.1: BrachyView probe concept and schematic representation

Semiconductor radiation detectors

Semiconductor pixel detectors are a particularly important class of radiation detectors, mostly due to their broad spectrum of applications. Although they were originally designed for high energy physics, they slowly found their way into different fields, due to their reliability, excellent resolution and cheap production cost.

Semiconductor radiation detector consist of arrays of semiconducting diodes with their electrodes depleted with a reverse bias. As ionizing particles strike the depleted volume of the detector, a charge is created which drifts towards the electrodes via the electric field. The collected carrier current is often integrated by the read-out electronic which is responsible for signal amplification, discrimination and analogue to digital conversion (ADC). Pixelated detector with individual electronic chains capable of signal processing for each pixel are referred to as Pixelated Hybrid Semiconductor Detectors. The hybrid device is composed of two chips, the sensor chip which is a semiconductor diode where the charge is deposited, and the readout chip which contains the electronics for all pixels and is bump-bonded to the first chip. An example of this type of detector is the Medipix2. —The monolithic devices are comprised of one chip, which acts as a sensor and performs a basic electronic readout through a source follower or a current amplifier. This type of device is referred to as DEPFET Macro-pixel detector and is developed in MPI Semiconductor lab in Munich, Germany.

Charge sharing is a common problem which affects pixel detectors, as the charge cloud created by the ionizing particles striking the surface of the detector are able to expand and travel through the face of the detector during the charge collection process. This originates

mainly from electrostatic repulsion and charge diffusion and poses difficulties as the charge can be collected by several adjacent pixels forming a cluster.

In detectors with a small pixel size and/or thick sensor, the original charge is almost never completely collected by a single pixel. The collected charge from the ionizing radiation is compared to a set threshold level and if lower, the charge is not registered and thus the charge is lost. Due to charge sharing, the charge registered over a number of pixels will usually be lower than the set threshold, which results in loss of the signal, and deteriorates the energy resolution. [19]

Medipix2

The Medipix collaboration developed a single photon counting pixel detector readout chip using a 0.25µm CMOS process. In high energy physics, hybrid pixel detectors are most desirable as they provide practically "noise free images" of particle collisions. These detectors typically work by using a preamplifier, which amplifies the charge deposited in a sensor, producing a fast-shaped pulse. This is compared to a set threshold, to then increment the counter. This type of detector is capable of imaging with practically no noise, which is the main interest in such devices.

The Medipix2 detector has a square surface which consists of a matrix of 256 x 256 square pixels each measuring 55µm on the side. The deposited charge, caused by the ionizing radiation, enters the pixel through the aluminium bump bonding pad. The charge is then, integrated on the feedback capacitor of the pre-amplifier. There are two set thresholds, and they can be adjusted within each pixel, this is to avoid pixel-to-pixel threshold variation. The amplified voltage is compared to the set thresholds and if it falls within its range, a single pulse is generated at the output of the double discriminator logic. An external shutter is applied to the chip, when this shutter is active the pulses from the double discriminator logic are then connected the clock of the pseudo-random counter within the pixel, resulting in each pulse incrementing the counter by one.

The standard chip is comprised of a single chip readout and a single sensor made of 300µm thick high resistivity Silicon which are connected via bump-bonding. The single chips can be assembled into different configurations allowing for larger detection areas serving different purposes. [20]

Timepix is the replacement detector to the Medipix2. Timepix has the same physical dimensions and features as the Medipix2 detector; with the added ability of each pixel to operate in three different mode: Medipix mode (counts the number of striking particles), Timepix mode (counter works as a timer and measure time of interaction) and Time-over-Threshold (TOT) mode, which allows for direct energy measurement in each pixel. Jakubek et al. studies the effects of charge sharing on the hybrid silicon pixel detector.

The charged collected within each individual pixel can be measure when the Timepix is operated in the TOT mode. The detector consists of 65536 individual pixels each with their corresponding and independent channels, with a non-uniform energy response. This obviates the need to calibrate each pixel. The calibration procedure uses pixel clusters of different sizes, neglecting the charge lost due to charge sharing to adjacent pixels. A detected particle creates a cluster of pixels, with its total energy equating to the sum of the calibrated responses of pixels in the cluster, plus the charge lost due to leakage. The lost charge will cause a distortion between different sized clusters, which was recorded experimentally. The

same process was investigated using simulations and the results agreed well with the experimental data.
There are three main factors that play a role in the charge sharing effect, the speed of the charge collection which is determined by the bias voltage, the deposited energy and the depth of particle interaction. A simple experiment was designed to study the influence of the interaction depth on charge sharing. A tilted detector was illuminated by X-ray photons through a slit (mimicking a point source), this set up allows for determination of cluster size on the depth of interaction. By analysing each recorded cluster separately, it was found that the average cluster size has a quadratic dependence on the depth of interaction. This result implies a linear relationship between average cluster radius and interaction depth. [21]

Medipix2 used in Radiotherapy

The development of cancer treatment methodologies based on hadron beams, such as ions and protons, is mainly due to their advantageous depth-dose distribution and the excellent radiobiological effective they offer. In Catania, Italy, the Istituto Nazionale di Fisica Nucleare - Laboratori Nazionali del Sud has been operating using a superconducting cyclotron which generates proton beams with a maximum energy of 62 MeV. For clinical use the beam passes through a series of modulators, range shifters and collimators. Quality assurance of the beam specifications is an integral procedure prior to any treatment period. The team at this centre have set out to develop a detection system based on the Medipix2.
The Medipix2 detection system was used as a single proton counting device, monitored by a control detection system based on a YAP:Ce scintillating crystal. This crystal was chosen due to its superior properties such as medium-high density, high light yield and fast response. The measurements taken by Medipix2 were accurately matched by the control system, which demonstrates its capability as a single proton counting device. Due to its fast acquisition time, this system can be proposed as a routine beam detection system. [22]

The Medipix2 offers many features that may be favourable for X-ray dosimetry. This detector allows noiseless photon counting which presents the opportunity to monitor low energy photons as low as 3.5 keV. The small pixel size allows for processing of high dose rates, and due to the large number of pixels, dosimetry at low does is also possible. Michel et al. has developed a system based on photon counting pixel detectors, such as the Medipix2, th at can determine personal dose equivalents from the number of counts in energy deposition intervals.
The Medipix2 is capable of detecting single photons with energies as low as 3-4 keV. This allows for the possibility of detecting a small number of photons with very low energies. It has been demonstrated that the surface dose delivered by very low energy photons increases with decreasing photon energy. An active personal dosimeter can examine the leakage radiation and therefore reduce the risk to the practitioners.
The aim of this study was to demonstrate the advantages of using personal dosimeters based on photon counting pixel detectors such as the Medipix2 when measuring personal dose equivalents for photon beams with energies below 150 keV. Although these detectors suffer from charge sharing which introduce defects in such dosimeters, they still prove to be capable of personal dosimetry. Due to the nature of development of Medipix2 being medical imaging, it does not have a problem detecting pulsed beams; this is an advantage of this system when compared to active personal dosimeters based on other detectors.

The Medipix2 has power consumption in order of several hundred mW, depending on counting and readout activity. Therefore, it is impossible to have continuous operations for extended periods of time. By using low power front-end in the pixel electronics, it will be possible for the photon detector to be used for several days without recharging.
A major problem with a Medipix2-based personal dosimeter, is the angle of incidence of the radiation. Only photon beams perpendicular to the detector will deposit their entire energy with in the sensor layer. This is due to the self-attenuation of the photons within the upper Silicon layer.
A personal dosimeter based on the Medpix2 has a number of benefits, such its small lower threshold of its energy range, its large range concerning dose rate and its very high statistical accuracy at low dose levels. [23]

Another application of Medipix in radiotherapy has been explored by CMRP for eye plaque brachytherapy. Radiotherapy is the most common type of treatment for posterior u~~n~~veal melanoma, and of the available radiotherapy treatment methods, the most preferred is brachytherapy. This is mostly due to the high cost and lack of widespread accessibility of its rival treatment type, proton therapy.
Eye brachytherapy typically uses I-125 or Pd-103 seeds, encapsulated within a Ru-106 for uniformly coated plaques. The TG-43 is the governing protocol for all brachytherapy calculations, it assumes an infinite body of water and does not account for an eye plaque. There exists a limited range of quality assurance techniques for customized plaques. By considering factors affecting the complexity of the treatment, for instance, the tumour size, shape and location, the surrounding vital tissue can be considered and spared.
A 3D dosimetry of the eye plaque will provide an improved QA for the eye brachytherapy treatment. Weaver et al. suggests the incorporation of a pixelated, silicon detector, the Medipix2, for the development of such a system. The importance of dose verification of the eye plaque is highlighted by the dose variability of the dose and misplacement of the seeds within the plaque. The study conducted the CMRP at University of Wollongong aims to improve the existing clinical QA for brachytherapy treatment through the development of a treatment plan evaluation system.
The effects of backscatter from the material positioned adjacent to the detector were studied to allow for optimal design of a QA system. Another focus of this project was to compare the event counting mode of the Medipix2 to the Time over Threshold mode on the Timepix for I-125 dosimetry. The total charge deposited in the sensor layer can be determined by running the Timpix in TOT mode.
Using the excellent imaging properties of the Medipix2 detector, Weaver et al. could determine the effects of backscatter to the dose received by the detector. This information is crucial for the improvement of the QA systems in place. They also determined that the TOT and count mode were significantly similar, and concluded that a dosimetry system based on the Medipix2 in event counting mode presents a cheaper and simpler alternative. [24]

Pinhole design and optimisation

In a comprehensive study of the pinhole size and shape at the CMRP s at the University of Wollongong, Alnaghy et al. set out to investigate pinhole geometry, more specifically, single-cone verses double cone design. An analytical model is further developed for a single cone pinhole, and its findings are validated using Monte Carlo simulations. This project was aimed at determining the optimal pinhole design to be used in the HDR BrachyView Project.

The most important parameters of a pinhole photon detection system are spatial resolution and sensitivity, which ideally should be as high as possible. In a pinhole system, the spatial resolution is defined in terms of the width of the Pinhole Response Function (PRF) exceeding a fraction (k) of its maximum value. The PRF is the 2D spatial distribution of the photons emitted by a point source and passed through the pinhole to reach the detector. The total sensitivity of the pinhole is determined by the sum of the geometric sensitivity which is the fraction of photons passing through the pinhole the pinhole aperture, and the penetrative sensitivity, which represents the fraction of photons attenuating through the collimator medium.

The analytical model was designed for a single cone geometry and compared to an existing equivalent model for a double cone geometry. The Monte Carlo simulations of a realistic point source model, agree with the theoretical values of the Full Width Half Maximum (FWHM) of the PRFs. The Penetrative Sensitivity of the double-cone pinhole system was shown to decrease more rapidly than the single cone system. This is particularly true for large horizontal displacement of the point source.

In the HDR BrachyView, the projections of centre of mass of the seeds is the most vital information acquired through the pinhole, its accuracy is very important to estimate the projection the centre of the source. The centre of mass for the true projected seeds is proved to be in good agreement with the Monte Carlo simulations for both pinhole designs for seeds contained in the full field of view. However, a much greater difference was observed for seeds nearing the edge of the field of view using the single cone aperture.

The double cone pinhole design was shown to have better sensitivity, spatial re solution and more capable of estimating projected centre of seeds, than its rival aperture design. The team at University of Wollongong appropriately concluded that the double cone pinhole was more suitable for the purposes of the HDR BrachyView probe. [25]

Chapter Four: 20 Seeds Experiment

The present chapter describes the main work performed in this thesis and published in the paper listed below. The candidate was the main person responsible for experimental setup, measurements during the experiment, reconstruction of the seeds and the analysis of the results. He also contributed to the writing some parts of the paper and producing most the images and tables present.

Alnaghy, S., Loo, K., Cutajar, D**., Jalayer, M.**, Tenconi, C., Favoino, M., Rietti, R., Tartaglia, M., Carriero, F., Safavi-Naeini, M., Bucci, J., Jakubek, J., Pospisil, S., Zaider, M., Lerch, M., Rosenfeld, A. and Petasecca, M. (2016). BrachyView: multiple seed position reconstruction and comparison with CT post-implant dosimetry. Journal of Instrumentation, 11(05), pp.P05002-P05002.

Materials and Methods

The original design of the BrachyView probe, is based on a multi-chip version of the Timepix detector, consisting of four separate sensors, aligned horizontally. The "edgeless" technology featured in the multi-chip, allows for maximum detection space, with a minimal dead layer of 25µm. Due to prolonged unavailability of a functioning multi-chip setup, for the purposes of this experiment a single chip Timepix detector was coupled with a single pinhole lead collimator. To mimic the multi-chip configuration, the single Timepix chip is translated in 15mm increments using a high precision stepper motor.
The collimator utilised in this experiment is constructed by hand from a flat patch of lead of 1.2mm thickness. It features a single cone-shaped pinhole with major diameter of 800µm and minor diameter of 200µm. An analytical proof of pinhole optimization was formerly done by Alnaghy et al. the shape and the size of the pinhole for this experiment was guided via the previous work done and experimental work using active I-125 seeds. [25]

The phantom used in this experiment was constructed at University of Wollongong, from Polymethyl methacrylate (PMMA). This material was chosen for its similar density to the body tissue and it clear structure. The phantom measures 60x60x60mm^3 and features a matrix of holes drilled through its length. The template used in this experiment is the CIVCO™ LDR Sterile 17GA Grid, for 1.3mm diameter open ended needles. In a clinical scenario this template provides a series of precisely placed needle guide channels, which enables accurate placement and insertion of the needles, in relation to the ultrasound imaging probe. In this study it was used for correct placement of the loaded needles into the phantom in relation to a clinical layout.

For the purposes of this experiment, twenty loose I-125 seeds (model 6711 Oncura) were acquired. I-125 Seeds feature a gold radiopaque marker in the centre which is enclosed in a thin layer of Aluminium and coated with a thin layer of Copper. The entire seed is encapsulated in a Titanium shell and measures approximately 4mm in length and 1mm in diameter. The activity of batch was examined using a well-type ionization chamber at the St. George hospital in Sydney pre-implantation. According to Australian College of Physical Scientists and Engineers in Medicine (ACPSEM) standards, devices used for clinical quality

checks need to be calibrated periodically, in intervals no longer than 2 years. For clinical purposes the activity of 10% of the batch or 10 seeds are measured, however to ensure the activity of all the seeds was in good agreement, the whole batch was tested. Each seed was placed in the insert of the chamber and measured twice, for 60 seconds, in each orientation, to ensure uniformity of the radioactive component within the source. Lead shielding was used to ensure radiation protection as the seeds were active.

The ACPSEM recommends that individual source activity verified by a well chamber needs to be within 3% for loose seeds. Considering this requirement, an average Air KERMA strength of 0.455 $\mu Gy\ m^2 h^{-1}$ was determined for the entire set of seeds. The treatment plan was devised by an experienced oncologist, and is based on a standard clinical scheme. As evident in Figure 4.1, the hypothetical location of the intra-prostatic urethra is not implanted. The needles were inserted in positions, B3, C2, c3.5, D2, E2 and F3. Table 1 demonstrates the loaded needle positions with the activity of the corresponding seeds. In a clinical setting the implantation process starts in the top left corner of the plan and progresses to the bottom right, this was the method of implantation employed with the following order: c3.5, d3.5, B3, F3, C2, D2, E2. Figure 4.1 displays the PMMA phantom with the inserted needles highlighted.

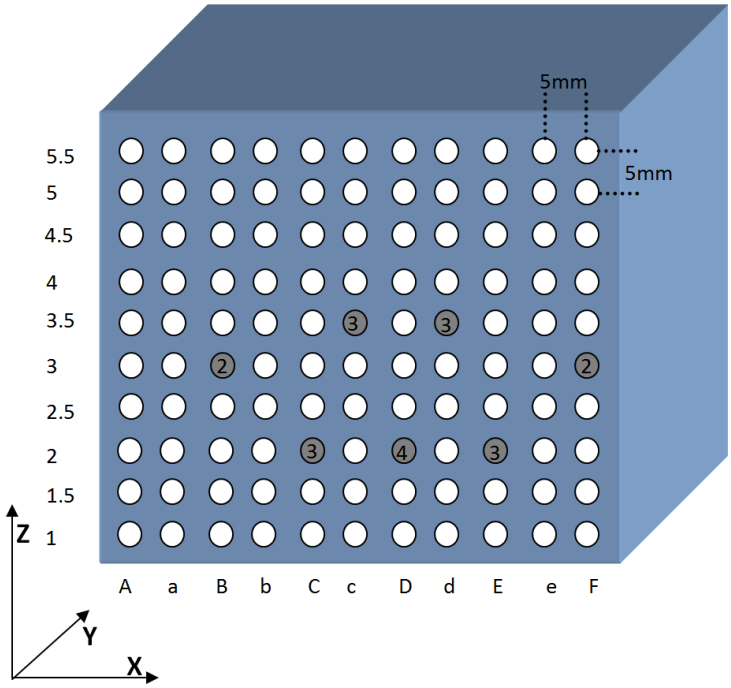

Fig. 4.1: Schematic showing 60x60x60mm^3 PMMA phantom with the positions of the 20 active seeds marked grey. The number of seeds within each needle is indicated. The same coordinate system is used for the identification of the seeds.

The images were acquired using a single Timepix detector, and were monitored during the implantation process in real-time. This demonstrated the capability of the system to identify individual seeds as they were implanted within the phantom. In a clinical scenario, there is a delay of approximately one minute between each needle implant, which reflects the abilities of an experienced oncologist. This time delay allows for the acquisition of the photons emitted by a set of seeds in each needle, via the gamma camera.

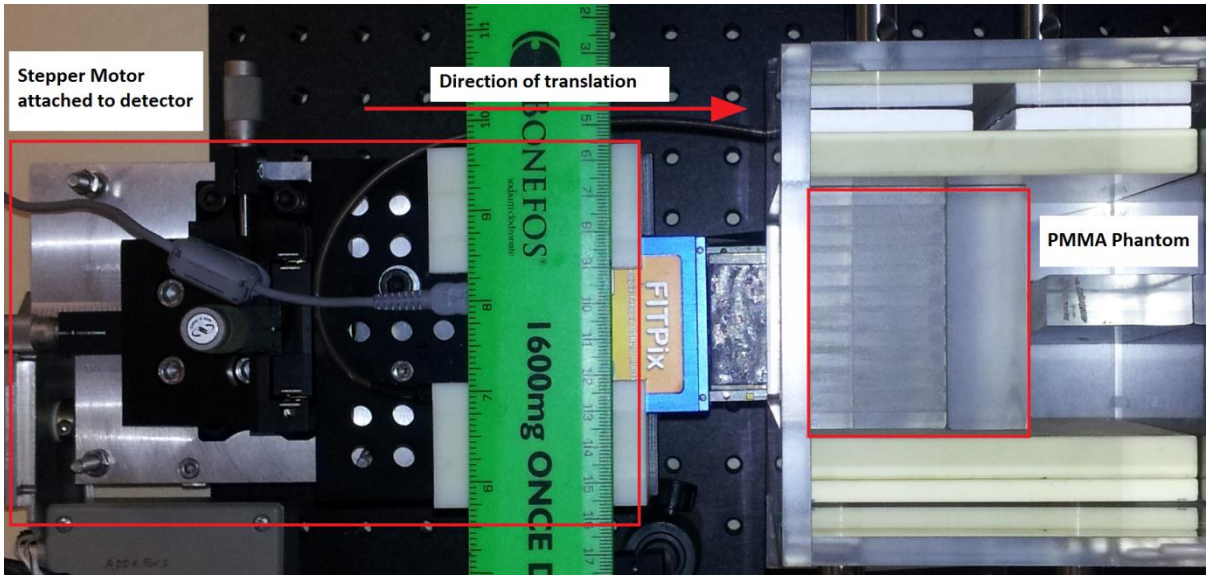

Fig. 4.2: Photograph of experimental setup taken from above, displaying the PMMA phantom with drilled holes and stepper motor with direction of translation.

The experiment took place in a CT scan room at the Cancer Care Centre within Sydney's St. George Hospital. A full CT scan was acquired using the medical CT scanner in the room, Siemens SEMATOM® Emotion, as the experiment was set up on the CT bed, the apparatus was not moved, eliminating motion errors in the results. To allow for a more accurate 3D reconstruction, a slice width of 0.8mm was used for the CT scan, in comparison a routine clinical CT 2mm thick slices. To emphasise "bone density", the images were post-processed, a CT number window between 400 – 1200 was used to highlight the shape and position of the implanted seeds. This also aids to reduce the effects of the artefacts introduced to images due to the material with high-density used in the experimental setup such as the optical bench pillars. Figure 4.2 and Figure 4.3 demonstrate the experimental setup in the CT operation room.

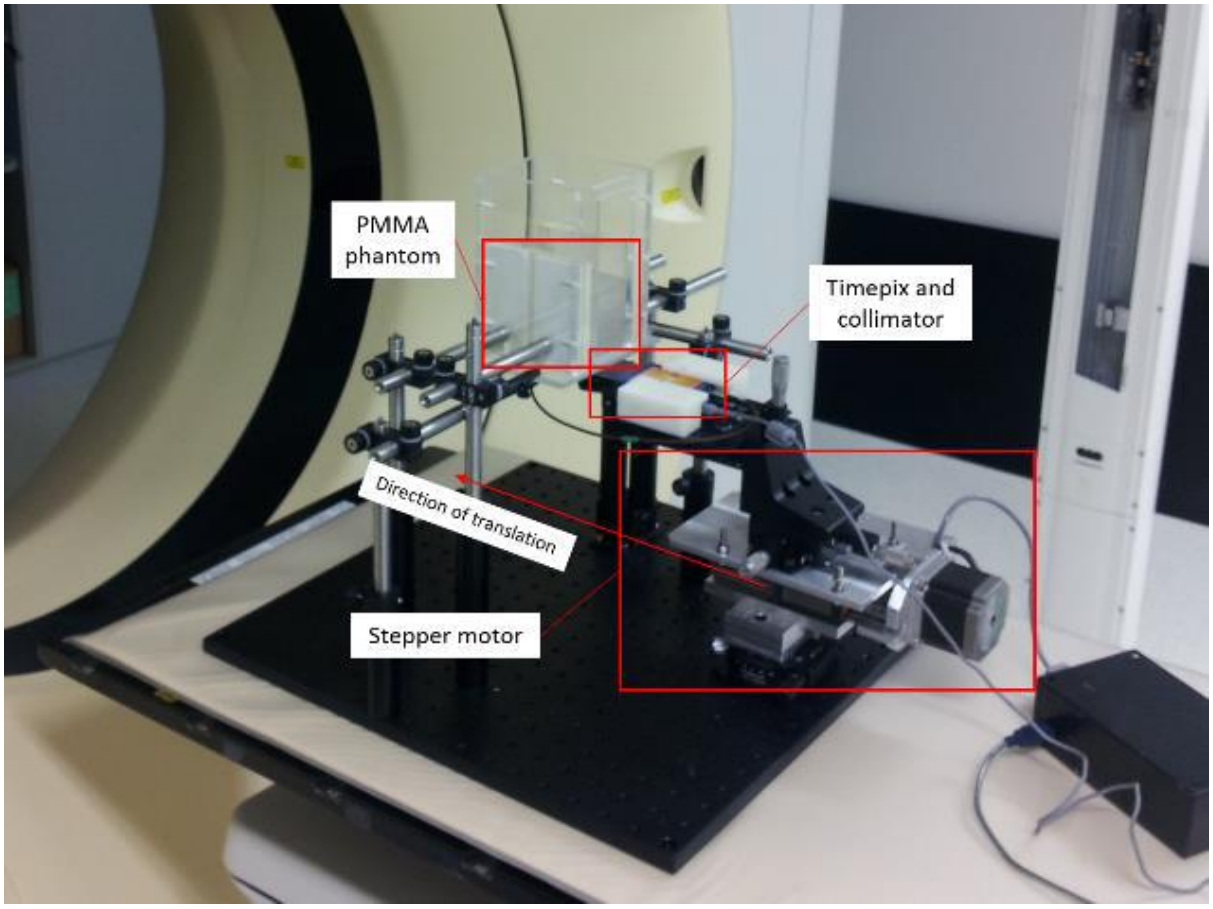

Fig. 4.3: The experimental set-up consists of the detector, the phantom and the high-precision stepper motor, fixed on an Aluminium optical Bench. The Experiment was performed at a CT suite room at the Caner Care Centre at the St. George Hospital

After each needle was implanted, the pinhole camera acquired three projections of the phantom in 15mm intervals, and a full CT was taken. The CT scan with all 20 seeds in place is used as a reference to verify the accuracy of the localisation of the seeds by BrachyView. The comparison of the two will verify the successfulness of the co-registration method utilised for the coordinates systems of BrachyView and the CT data set.

The detector and pinhole collimator were aligned using an active seed directly above the pinhole collimator and altering its position until its projection fell on the central pixel. A similar process was used to align the pinhole camera with the phantom, this time with the seed placed in the D2 position of the PMMA phantom and adjusting its position using the high precision stepper motor. The coordinate system of the gamma camera $(\mathrm{x}, \mathrm{y}, \mathrm{z})$ with its origin defined as the pinhole. The high precision stepper motor translates along the Y axis of this system.

The datasets from the BrachyView and the CT were co-registered using a point-to-point method. A new origin has to be selected at a point where both the datasets can be represented by an appropriate rigid shift and rotational transformations. This will be at the midpoint of the line between the two markers which can be easily identified in both data sets. The seeds in positions B2 and F2 (the outermost seeds in the phantom) were chosen as the markers in this study. The coordinates of all the seeds were calculated with respect to the registered origin.

The effects of seed misplacement on the dosimetry were assessed via TG-43 based calculations performed on the experimental brachytherapy seed plan. These dose calculations used the positions of the seeds determined by the BrachyView and the CT. To determine the effects of localisation discrepancies, several comparison studies were carried out, including 2D Isodose Comparisons (2DIC), 2D dose difference colour-wash and dose volume histograms (DVH) of the CTV. The total treatment dose (after full decay) from all seeds were superimposed on 700x700 pixel grid (representing a 7x7cm^2 field) to create the isodose curves, following TG-43 guidelines. If the determined dose was within a ±5% range of the prescribed dose, the pixel colour was changed to match the selected isodose colour.
Within every pixel location, the total dose calculated from using the CT seed distribution was subtracted from the total dose from the seed distribution determined by the BrachyView to create the 2D dose colour-wash plots. Using an adjustable dose discrepancy scale, a colour value was selected for each pixel.

Three-Dimensional Reconstruction

This experiment is aimed to test the probe using a larger number of seeds (20 active seeds) within a more clinically relevant scenario. Triangulation is used to calculate the coordinates of the centre of mass of each seed, and the positions of the seeds within the phantom can be reconstructed.
Triangulation is a conventional three-dimensional reconstruction technique, which uses two dimensional projections of the object, to find 3D coordinates of the point of interest. This method requires at least two sets of projections for reconstruction. Triangulation is an excellent tool for rigid 3D reconstruction and is relatively computationally efficient.

The back-projection method utilised, uses the 2D images generated by the incident gamma rays from the seeds projected onto the sensor plane through the pinhole collimator. The pinhole is defined as the origin of the camera frame (X_{c0}, Y_{co}), the image of a 3D object (i.e. I-125 seed) is projected through this pinhole, on a 2D detector plane. To make matters simpler, the centre of mass (COM) of the seeds is taken to approximate their position, ignoring at this stage, their orientation.
To mimic a triple chip Medipix detector each equipped with their identical corresponding pinholes, the single chip is translated via a drive system. This allows for three projected images of the COM which are then back projected through their respective pinholes, however only two projections through the pinhole collimator at two different positions are required to perform the reconstruction.
A simple mathematical model was developed to represent the relationship between the coordinates of the "3D point" P_c in the pinhole camera frame (X_c, Y_c, Z_c) and its projection P_1 onto the image plane (x, y) (Figure 4.4). The equation below expresses the relationship between (X_c, Y_c, Z_c) and (x, y) by the focal length $f_x = f_y = f$ assuming no astigmatic aberration in the system (square pixel size, square pixel array, cylindrical symmetry of the pinhole):

$$x = f\frac{X_c}{Z_c}, \qquad y = f\frac{Y_c}{Z_c}$$

If the origin of the image coordinate system has shifted from the centre of the image plane, the displacement (s_1, s_2) will be included in the projection equations (the parameter s_i can be used to represent any movement of the point P_c relative to the pinhole):

$$x = f\frac{X_c}{Z_c} + s_1, \qquad y = f\frac{Y_c}{Z_c} + s_2, \qquad z = Z_c$$

The above relations can be reformulated, using projective geometry framework as:

$$(\alpha x, \alpha y, \alpha)^T = (fX_c + s_1, fY_c + s_2, Z_c)^T \rightarrow \overline{P_1} = \mathrm{H}\overline{P_c}$$

Where $\alpha = Z_c$ is the homogeneous scaling factor, H is the intrinsic conversion matrix composed by the parameters which characterize the pinhole-image apparatus in the camera frame.

This model was implemented in MATLAB with the intrinsic parameters set to the experimental setup values. Using MATLAB algorithms in three-dimensional geometry, vector lines are drawn from the seeds' projections on the detector plane, through the pinhole for each detector position. The three detector positions will produce three vector lines as illustrated in Figure 4.5. Theoretically the coordinates of the intersection of these vector lines will be the position of the seed, however in three-dimensional space, non-parallel lines do not necessarily intersect. Therefore, a chord is extended in the closest path between vector lines from detectors 1 and 2, and from detectors 2 and 3. The average of their midpoints is considered as the position of the seed. The algorithm will also work using only two projections and thus two projected lines, however the added vector lines improves the accuracy of the system.

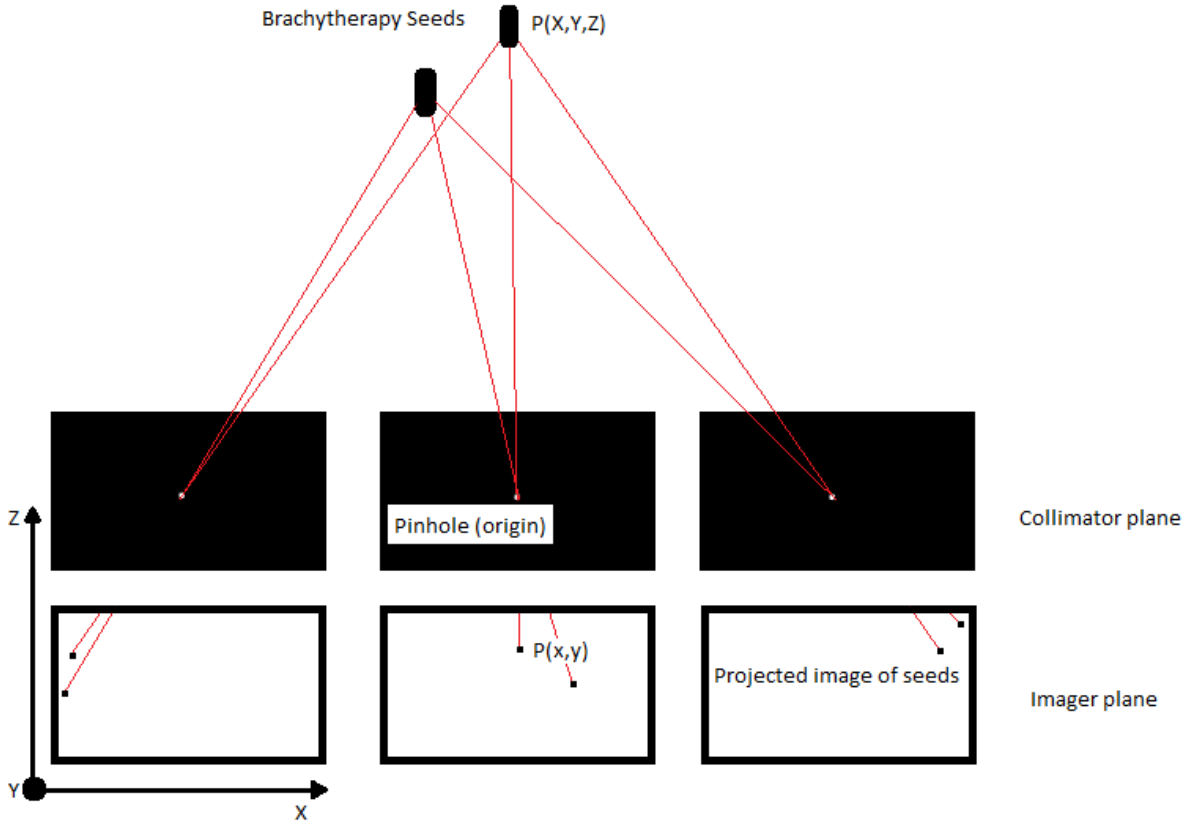

Fig.4.4: Schematic representation of the BrachyView coordinate model and reconstruction method by triangulation.

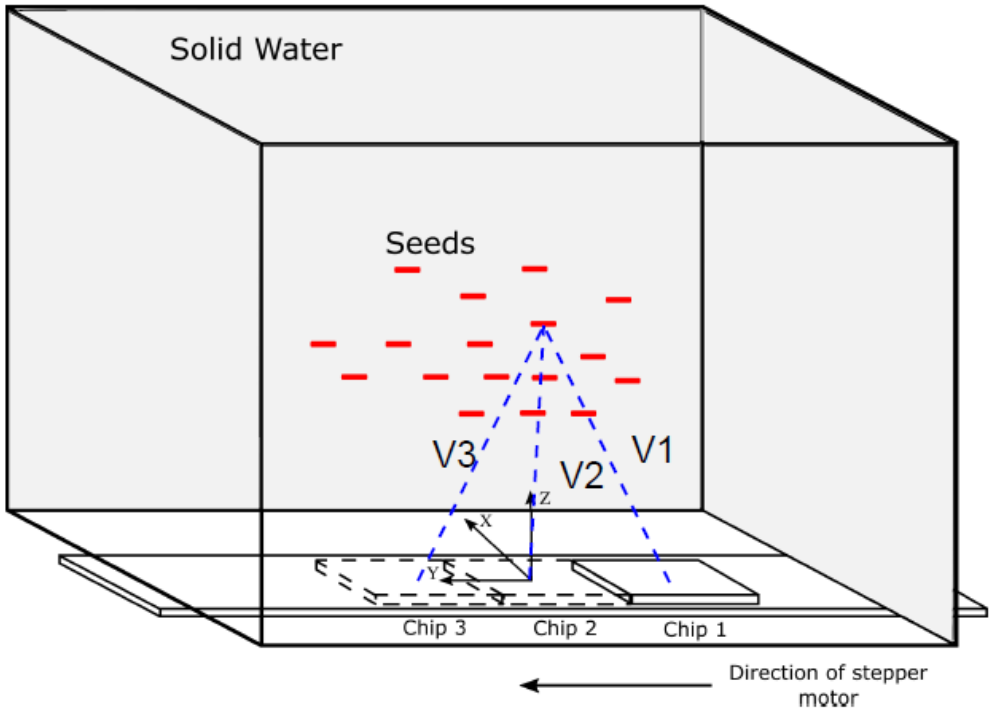

Fig.4.5: The experimental setup of the PMMA phantom and the direction of detector translation with the BrachyView coordinate system. Theoretical vector lines are drawn from an arbitrary seed through the pinholes.

Results

The progressive needle implantation procedure is captured by BrachyView, the projections in Figure 4.6 were obtained with the probe at its first position, corresponding to Y=0 mm.
Due to the scattering interactions in the phantom and the collimator, there is a noticeable increase in background noise and a gradual increase in counts detected. The detector is easily able to resolve the projections from all 20 implanted seeds, even with the increasing background noise. The order of implantation of the needles and the positions of the seeds is displayed in Table 4.1.

Order of Implantation	**Position CIVCO™ LDR 17GA Grid**	**Individual seed position in the needle and corresponding Air Kerma Strength (U=µGy m2/h) – Uncertainty ±1%**						
Needle #1	C2.0	0.44	SPACER	0.47	SPACER	0.45		
Needle #2	E2.0	SPACER	0.46	spacer	0.45	SPACER	0.47	
Needle #3	B3.0	0.45	SPACER	0.44				
Needle #4	F3.0	0.45	SPACER	0.43				
Needle #5	c3.5	0.47	SPACER	0.46	SPACER	SPACER	0.45	
Needle #6	d3.5	0.47	SPACER	SPACER	0.44	SPACER	0.45	
Needle #7	D2.0	0.45	SPACER	0.47	SPACER	0.46	SPACER	0.43

Tab.4.1: The seed positions within the needles and the order of implantation.

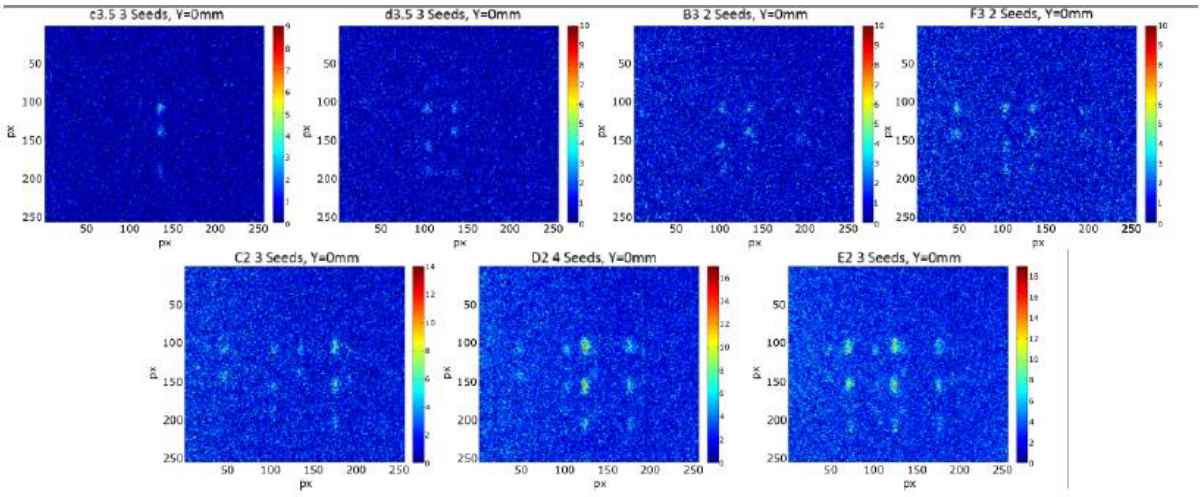

Fig.4.6: The projections captured by the pinhole camera highlighting the order of implantation intra-operatively.

As mentioned in the method, the experiment was carried out using a single detector placed below a single pinhole, and translated along the Y direction to mimic the triple chip setup. The projections are acquired at Y = -14 mm, Y = 0 (starting position) and Y = +14 mm, each seed can be identified in all three images. Figure 4.7 shows three projections of the whole set of seeds, with cross identifying the COM of each seed.

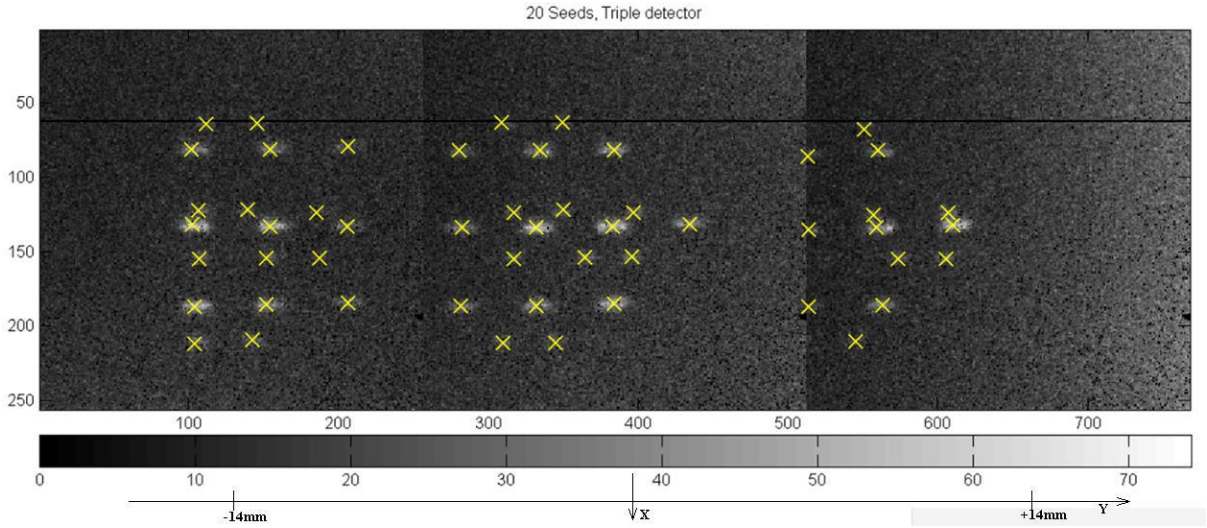

Fig.4.7: The triple chip detector image is obtained by stitching projections acquired at each Y position. Using the lateral shift of the detector (±14mm) and the seeds' projections, the 3D positions of the seeds can be reconstructed.

By using the new origin, the midpoint between the two selected seed markers (B3 and F3) the 3D reconstructed results from the CT and the BrachyView can be compared. These positions are superimposed in the graphs in Figure 4.9.

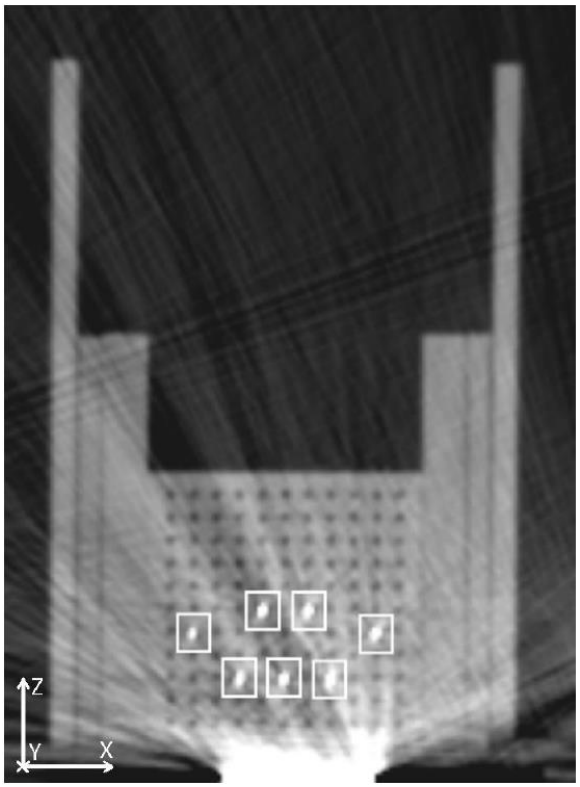

Fig.4.8: A transversal CT slice showing all 7 needles implanted, this is taken at the theoretical depth of the prostate base.

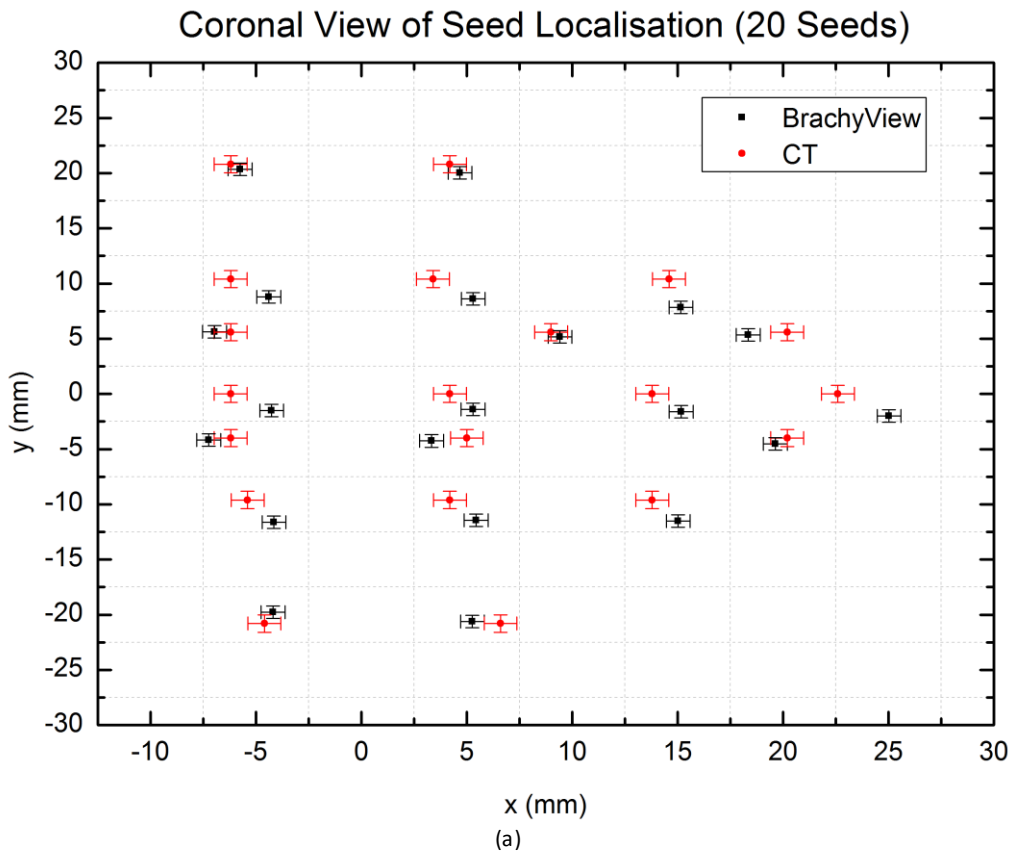
Coronal View of Seed Localisation (20 Seeds)
BrachyView
CT
y (mm)
x (mm)
30
25
20
15
10
5
0
-5
-10
-15
-20
-25
-30
-10
-5
0
5
10
15
20
25
30

(a)

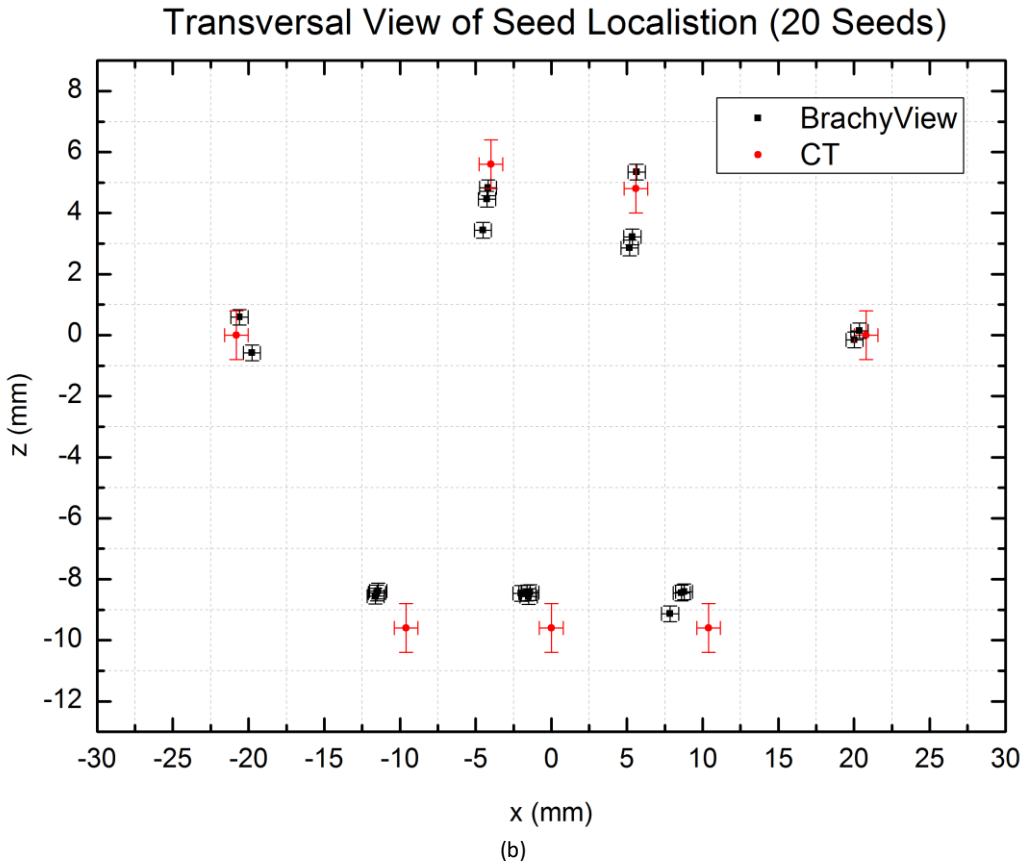
Transversal View of Seed Localistion (20 Seeds)
BrachyView
CT
z (mm)
x (mm)
8
6
4
2
0
-2
-4
-6
-8
-10
-12
-30
-25
-20
-15
-10
-5
0
5
10
15
20
25
30

(b)

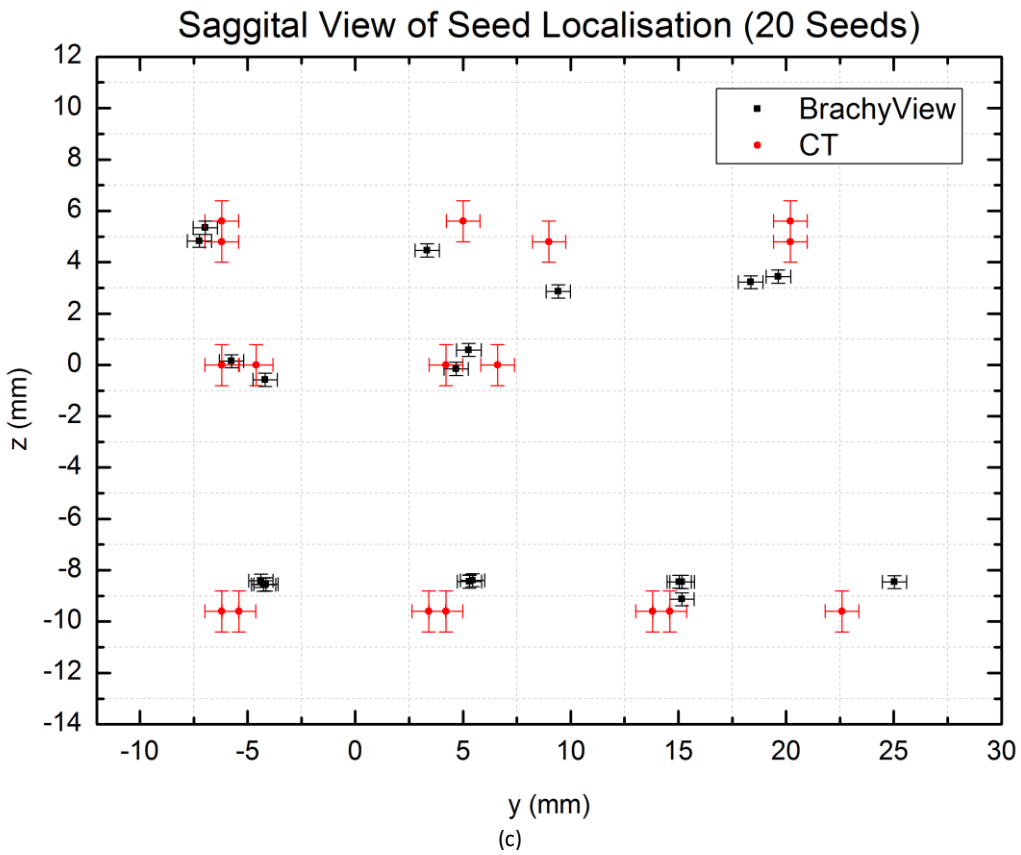

(c)

Fig.4.9: The 3D reconstructed positions of the seeds using the BrachyView and the CT are shown in orthogonal projections, in (a) top view (corresponding to XY), (b) front view (corresponding to XZ), and (c) side view (corresponding to YZ).

To better demonstrate the accuracy of the seed localisation, an additional visualization method has been utilised, a reconstruction of the seed population using the COM of the seeds resolved by the BrachyView. The model is based on the known shape and dimension of the seeds. The three-dimensional CT images are co-registered with the reconstructed images from the BrachyView. A high selective CT number is applied to the reconstructed CT images in order to segregate the high-density titanium cells of the seeds.

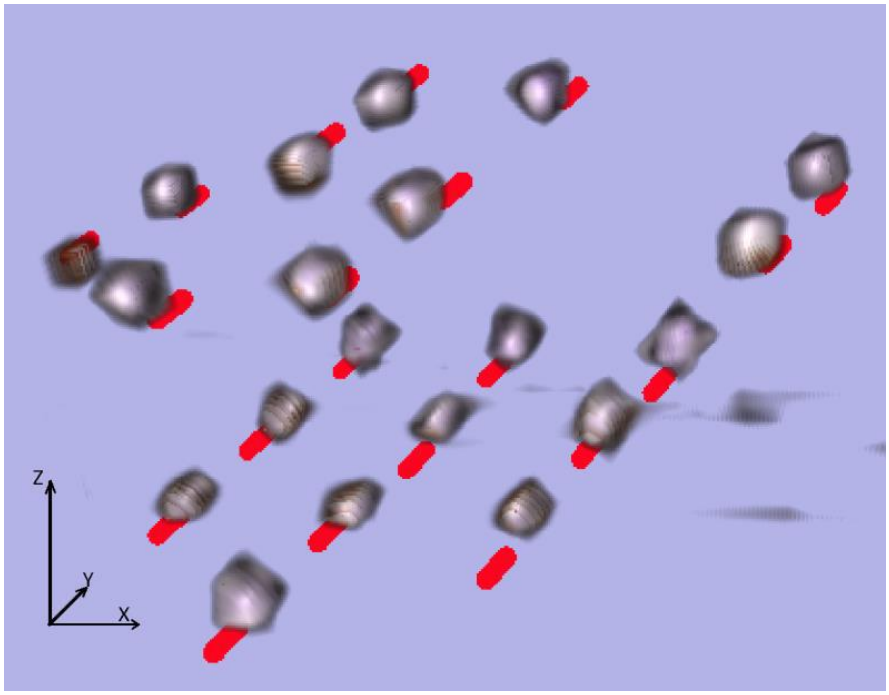

Fig.4.10: The co-registered images from the BrachyView and the CT scans, reconstructed in 3D.

The isodose calculations of the seeds localised by the BrachyView and the CT at depths y = 10 mm, y = 15 mm and y = 20 mm are shown in Figure 4.11 (a), (b) and (c) respectively. The BrachyView isodose curves are marked red and the CT isodose curves are marked blue. The DVH plot in Figure 4.12 compares BrachyView and CT determined seeds positions for a 50Gy prescription dose to Prostate CTV. As above the red curve represents the DVH for the seeds localised by BrachyView and blue curve for the CT determined seed locations.

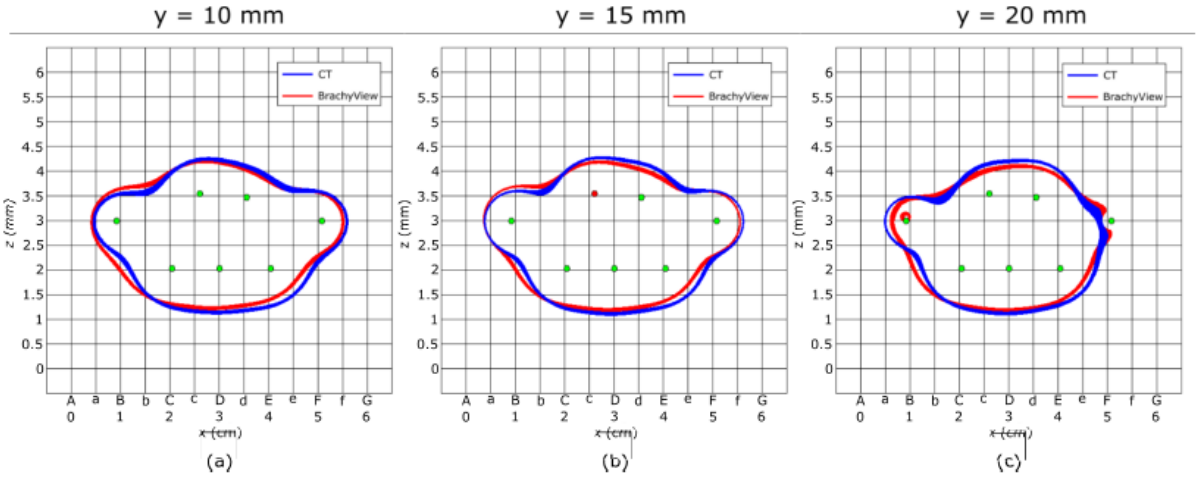

Fig.4.11: Comparison of the Isodose curves, calculated based on the locations of the seeds determined by BrachyView and CT. These isodose curves are taken at three depths at y = 10 mm, 15 mm and 20 mm in respect to the BrachyView coordinate system.

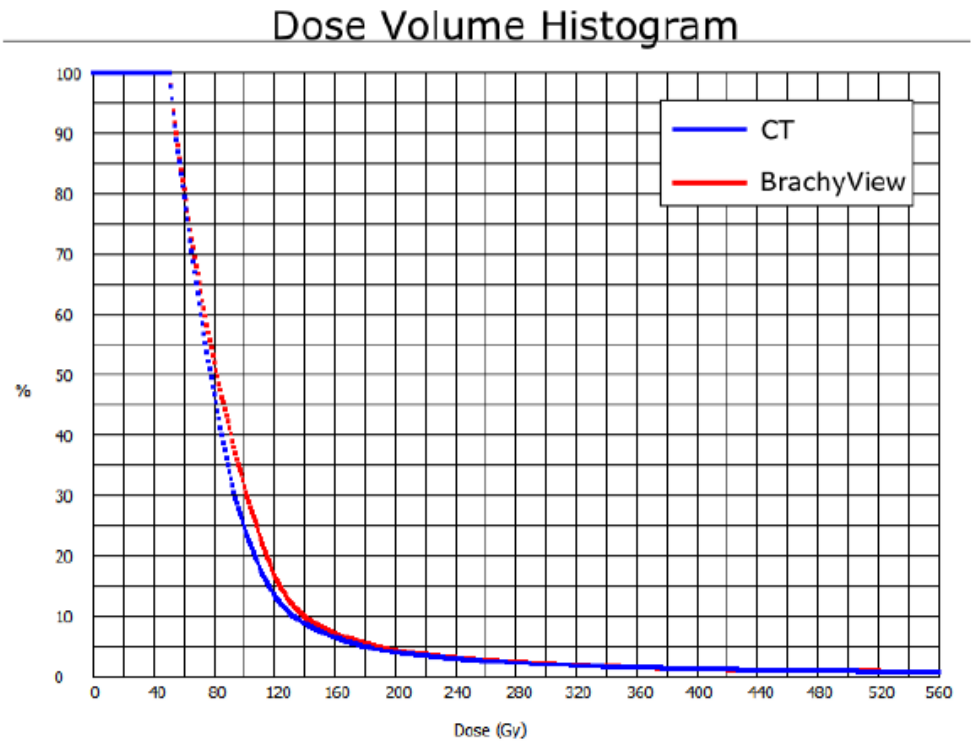

Fig.4.12: Dose Volume Histogram plot based of BrachyView and CT determined seed positions for a 50 Gy prescription dose.

An increase the in the background counts is expected with an increased number of implanted seeds. A subtraction method has been developed to account for this: after each needle is implanted, the frame (f) is recorded by the detector and a new frame $(f+1)$ is initiated. To clearly identify the seeds implanted during frame $(f+1)$, the count map from (f) is subtracted from this frame, resulting in the net pixel count map. This subtraction method follows the implantation procedure, and maintains an almost constant background signal despite the increase in the number of seeds. The developed algorithm is as follows:

$$g(i,j) = f_{n+1}(i,j) - \left(f_n(i,j) + \frac{f_n(i,j)}{t_n} \times t_{n+1} \right)$$

Where $f_{n+1}(i,j)$ represent the 256×256 pixel frame array at the n^{th} frame number, t_n represents the acquisition time of the n^{th} frame and $g(i,j)$ is the outputted subtracted frame.

The background signal will start to deteriorate the reconstructed image, with an increasing number of seeds implanted. Figure 4.13 demonstrates a linear increase in the background pixel counts per pixel per minute as more seeds are implanted. By extrapolating this trend in Figure 4.14, it can be estimated that the background to signal ratio will become a notable problem at around 30 implanted seeds. At this point the subtraction algorithm will be needed to maintain a steady signal to background ration for seed reconstruction.

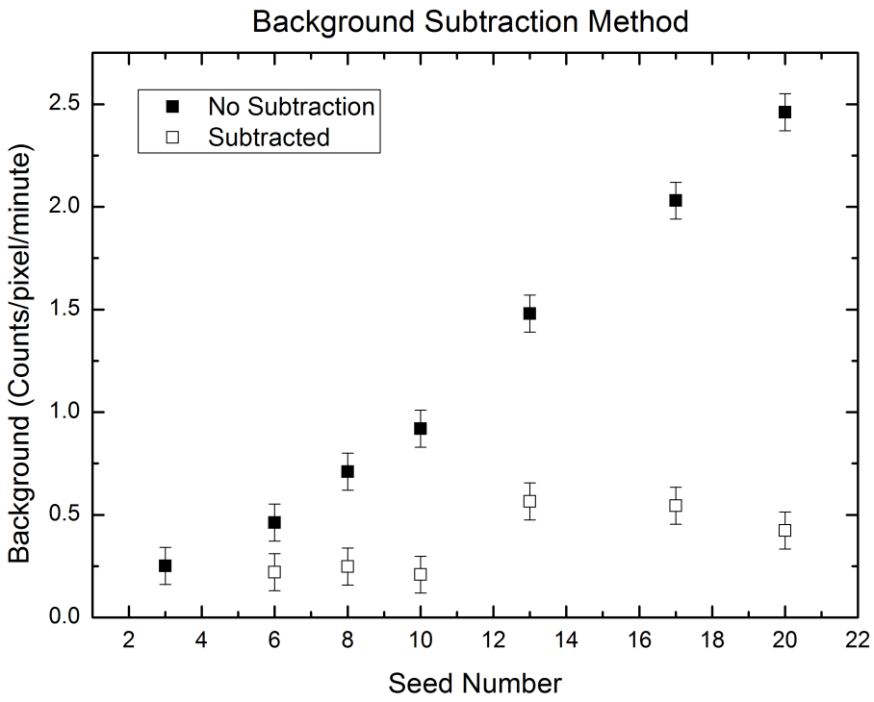

Fig.4.13: Increasing background signal with number of seeds, much improved signal to noise ratio with Background subtraction.

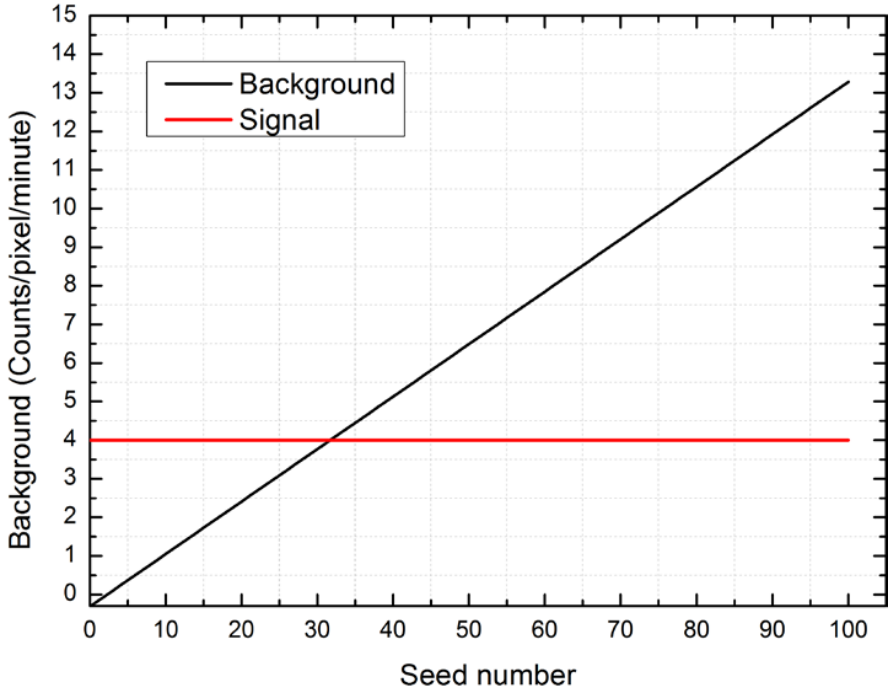

Fig.4.14: Linear extrapolated background noise demonstrating the need of the subtraction algorithm for more than 30 implanted seeds

Chapter Five: Gel Phantom Experiment

The following chapter describes the extension of the methodology developed and described in Chapter 4 to a gel phantom which better represent the elasticity and deformability of the soft tissues involved in LDR brachytherapy. In this work, the candidate has participated in the experiments and preparation of the setup.

The results of this experiment have been published on:
Alnaghy, S., Cutajar, D., Bucci, J., Enari, K., Safavi-Naeini, M., Favoino, M., Tartaglia, M., Carriero, F., Jakubek, J., Pospisil, S., Lerch, M., Rosenfeld, A. and Petasecca, M. (2017). BrachyView: Combining LDR seed positions with transrectal ultrasound imaging in a prostate gel phantom. Physica Medica, 34, pp.55-64.

Materials and methods

The original triple chip set up of the BrachyView probe was constructed for this experiment. The probe has a total length of 80mm and consists of a 1mm think cylindrical tungsten collimator enclosing a triple chip Timepix detector. The tungsten tube features three single cone pinholes located 22.5mm apart from each other with and opening of 112°, a physical diameter of 0.5mm and a channel length of 0.1mm, illustrated in Figure 5.1. A 4.5mm gap exists between the each Timepix sensor and its corresponding pinhole. Each chip consists of 256 × 256 pixels which give a total imaging area of 256 × 768 pixels. The PCB protruded the tungsten shell where the Fitpix readout system was made. A thin layer of Kapton was used to water seal the probe and to reduce the low-energy electron backscatter from the tungsten surface.

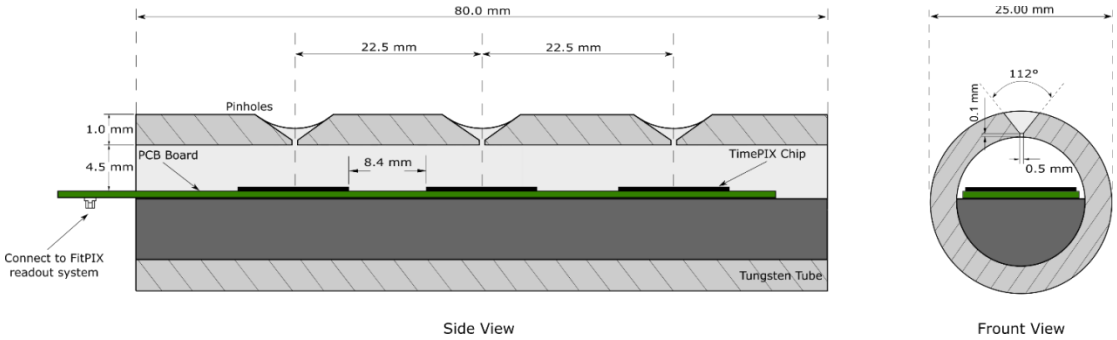

Fig.5.1: Design of BrachyView probe, incorporating three Timepix detectors housed in a 1 mm thick tungsten tube.

The phantom used in this experiment was CIRS tissue equivalent ultrasound prostate phantom. The CIRS Model 053-I training phantom specifically developed for practicing permanent seed implantation procedures. This phantom features a transparent gel to permit visualization of the orientation the probe and the implanted needles. The phantom was mounted on a PMMA stand which allows for position adjustment while creating a rigid setup to prevent mechanical movement during the treatment procedure. The experimental setup is demonstrated in Figure 5.2. The experiment was based on a clinical protocol for LDR brachytherapy treatment. The TRUS was first used to find the base of the prostate volume then it was stepped 5 mm deeper beyond the base, which defined the origin of the TRUS system. The entire prostate volume was imaged using 2.5mm slice increments until the phantom was completely covered.

There were 11 needles loaded with 30 active 0.4 mCi I-125 source, they were implanted into the prostate phantom with the aid of the TRUS guidance. Figure 5.3 shows the treatment plan utilised for this experiment. After the insertion of each needle the TRUS probe was removed and the BrachyView was inserted in the phantom cavity. Acquiring an image after each needle insertion allows for understanding cumulative counts of the implanted seeds. The BrachyView probe was carefully placed in the cavity such that the middle pinhole was aligned with the middle of the prostate volume. After all 30 seeds were implanted, a full CT scan of the setup was performed with the BrachyView probe inserted, using the Philips Brilliance CT system.

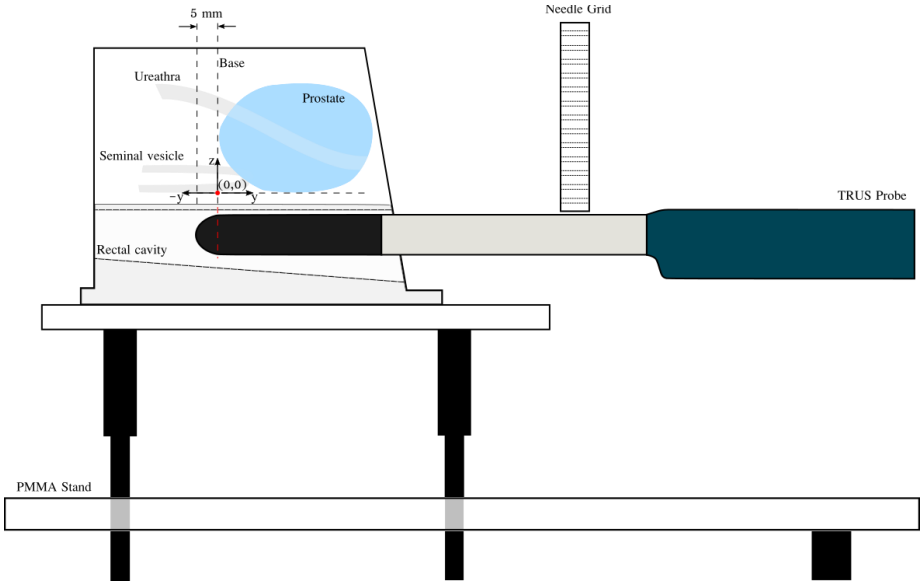

Fig 5.2: Experimental setup showing CIRS tissue equivalent ultrasound prostate phan-tom and TRUS system placed on PMMA holder.

Needle Number	Retraction (cm)	Hole Location	Number Seeds
1	*0.00*	*b3.5*	*3*
2	*0.00*	*E3.5*	*3*
3	0.00	B3.0	2
4	0.00	F3.0	2
5	0.00	C2.0	3
6	0.00	D2.0	4
7	0.50	E2.0	3
8	0.50	b2.5	3
9	0.50	e2.5	3
10	0.50	C4.5	2
11	0.50	d4.5	2

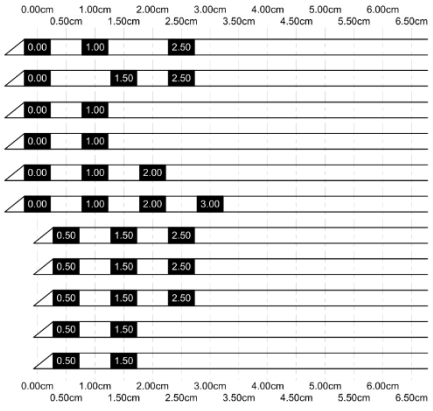

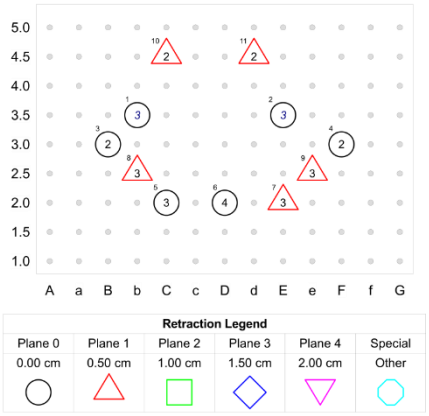

(a) (b)

Fig.5.3: Varian Medical Systems VariSeed treatment plan, (a) Needle loading table, showing planned seed positions for 30 0.400 mCi 125I seeds. (b) 2D grid of needle implant, showing plane location of first seed.

The basis of the reconstruction system remains the same for localising the position of the implanted seeds in the 3D. Using the triple chip mechanism, there is no need for translation of the probe and the projections are acquired simultaneously through 3 separate pinholes as illustrated by Figure 5.4. However, the COM of the seeds is calculated using a cluster recognizing algorithm, which is an improvement on manual selection of the seeds. The origin of the BrachyView system is selected as the corner of the first Timepix chip. Three vector lines

can be acquired from each seed projection; however, a minimum of two vector lines is sufficient to perform triangulation.

To find the minimum distance to all the vector lines, firstly an arbitrary point P with coordinates $(\mathrm{x}, \mathrm{y}, \mathrm{z})$ is considered. The perpendicular distance from the acquired vector lines $d_n$to point P is determined by:

$$|\overrightarrow{h_n}| = \frac{\overrightarrow{B_nP} \times \overrightarrow{d_n}}{|\overrightarrow{d_n}|}$$

By summing all these perpendicular distances, a function $f(x, y, z)$can be formed. Thus by minimizing f the intersection of all back projected line in 3D space can be determined.

$$f(x, y, z) = \sum_{i=1}^{n} \overrightarrow{h_n}$$

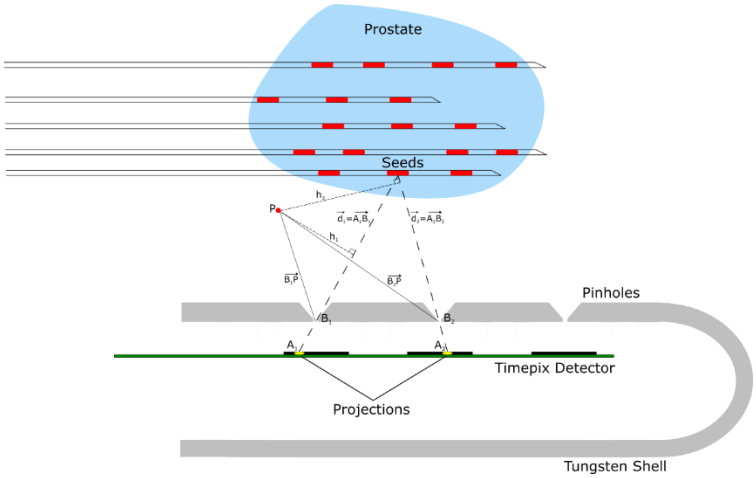

Fig.5.4: Conceptual view of reconstruction method for 125I seeds within a prostate volume.

The Nelder-Mead method is implemented here, to find the point with the smallest distance from all the vector lines. This method only uses function evaluations (i.e. no derivatives) thus is an iterative optimization technique starting at point P. It utilizes a Simplex, which is a polytope in N dimensions with N+1 vertices, in the case of 3D Cartesian coordinates system, is a tetrahedron which changes its shape until a minimum solution is located.

A software application has been developed specifically for the BrachyView system, which implements the reconstruction algorithm automatically. The need for manual selection of the seeds projections is eliminated, which had proved to be a tedious and time consuming task. The 3D interactive platform allows for the visualization of the treatment volume the brachytherapy seeds in a single coordinate system. The software was developed using Microsoft Visual studios and QT Creator in C++. The application is capable of rendering a 3D volumetric reconstruction of the prostate, using raw ultrasound slices. It utilizes external C++ libraries, Insight Segmentation and Registration Toolkit (ITK) and Visualization Toolkit (VTK), which are open source software tools for image analysis, 3D reconstruction and visualization for medical imaging purposes.

The raw ultrasound images are taking from the TRUS system as a bitmap file, and the application recognizes and extracts the prostate volume as a Region Of Interest (ROI). The gridlines overlaid by the TRUS software are removed and are replaced by using linear interpolation of the surrounding pixels. This process is necessary prior to the reconstruction, as the gridlines would appear to be planes through the prostate volume. The entire process is automated and requires no input from the user. Next a smooth 3D reconstruction of the TRUS images is acquired, by stacking the 2D ultrasound images in the z direction and performing linear interpolation. The dimensions of the LDR I-125 seeds are used to create a 3D representation of the sources. By loading the reconstructed positions of the seeds in the TRUS coordinates system, a 3D image the prostate with the LDR seeds overlaid is constructed. At the end of the implantation process, a full CT of setup was performed using a Philips Brilliance CT system. A slice thickness of 1mm was selected with an overlap of 0.5mm. To reduce the streaking artefacts from the tungsten collimator, Metal Artefact Reduction for Orthopaedic Implants (O-MAR) was selected. The CT scan is an accurate tool for comparison of the reconstruction data from the BrachyView, and is used as a reference. The CT data was also used to co-register all three coordinate systems of the CT, BrachyView and TRUS.
The origin of the CT coordinate system is the bottom right corner of the imaging volume, the origin of the BrachyView coordinate system is the corner of the first Timepix chip and the origin of the TRUS coordinate system is located 5mm from the base of the prostate and on the bottom right edge of the prostate volume. The positon of the BrachyView probe and the TRUS system was found relative to the origin of the CT coordinate system. Thus vectors were drawn from the origin of these systems, to the origin of the CT coordinate system, and were used to transform the BrachyView reconstructed seed positions into the TRUS coordinate system. The same method was used to transform the seed positions form the CT in the TRUS system. The CT data was also used to assess the accuracy of the 3D reconstruction of the prostate volume using the 2D ultrasound slices. Figure 5.5 illustrates a co-registration of all three coordinate systems.

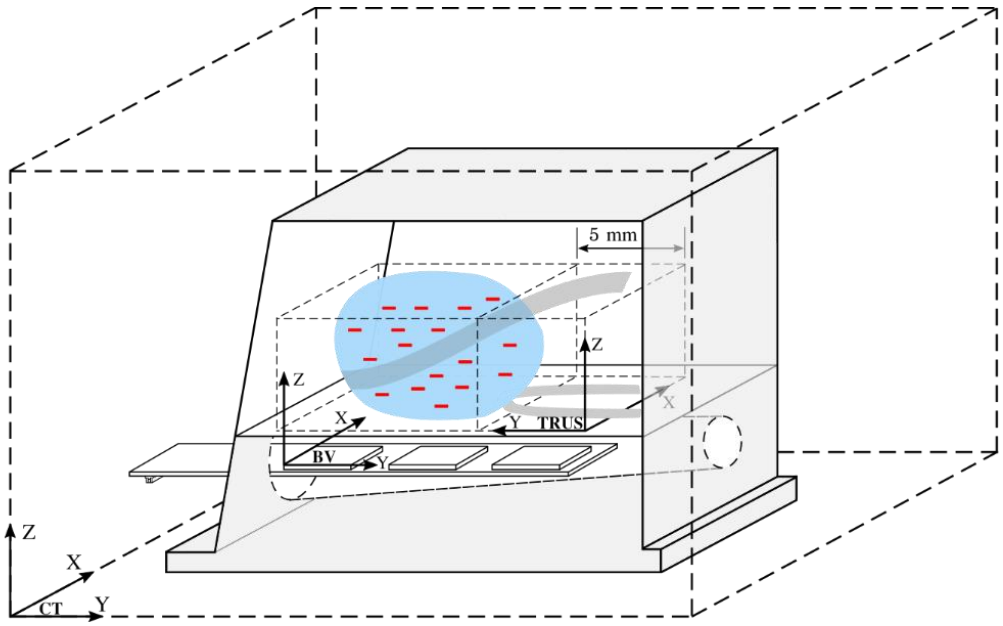

Fig.5.5: shows CT, BrachyView and TRUS coordinate systems based on experimental setup.

Results

The seed positions, determined by the CT images and reconstructed via BrachyView data, are plotted in Figure 5.6 in the three planes of the BrachyView coordinate system. Figure 5.7 illustrates a 3D scatter graph of the seed locations reconstructed by the CT and the BrachyView. Figure 5.8 shows screen shots of the developed software visualization interface at various viewing angles, displaying a 3D reconstructed prostate volume, from the ultrasound slices via the TRUS. Reconstructed LDR seeds from the BrachyView and the CT data set are co-registered on the 3D TRUS prostate volume (TRUS coordinate system).

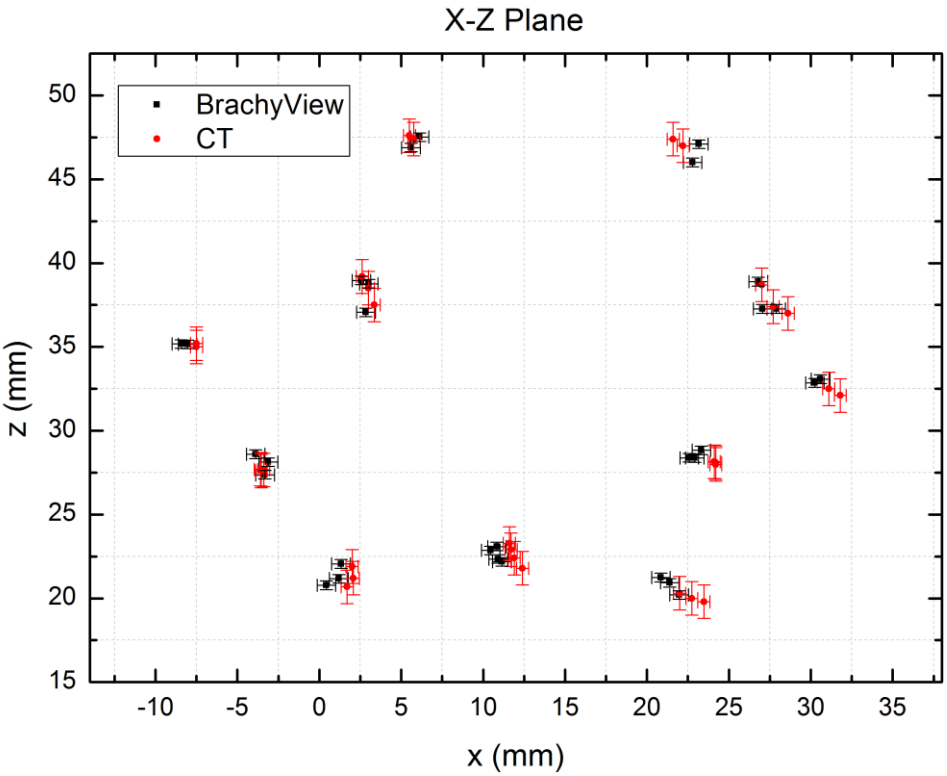

(a)

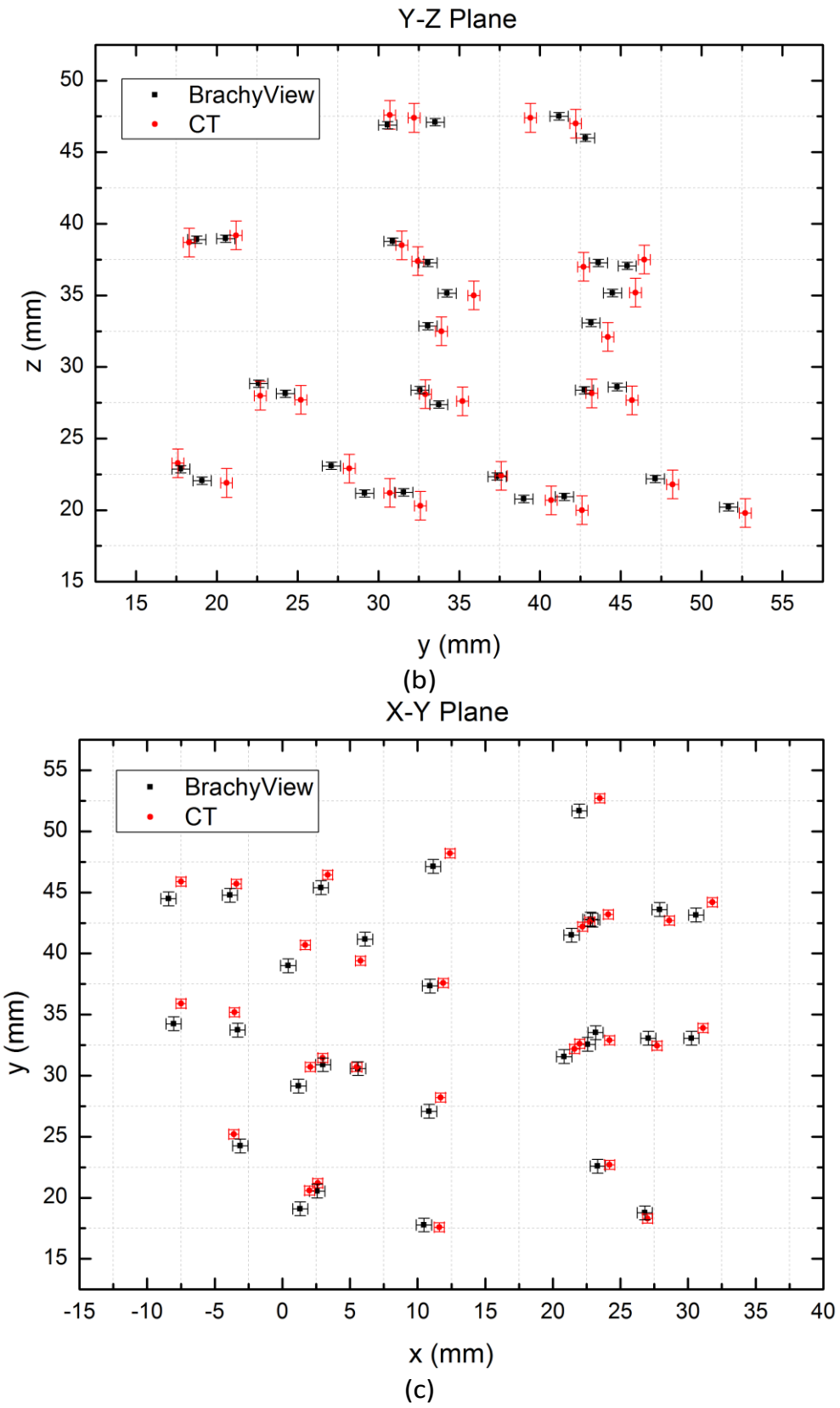

Fig.5.6: 2D scatter plots of reconstructed seed positions from BrachyView system and CT determined seed positions co-registered in the BrachyView coordinate system on each coordinate plane. (a) front view (corresponding to XZ), (b) side view (corresponding to YZ) and (c) top view (corresponding to XY).

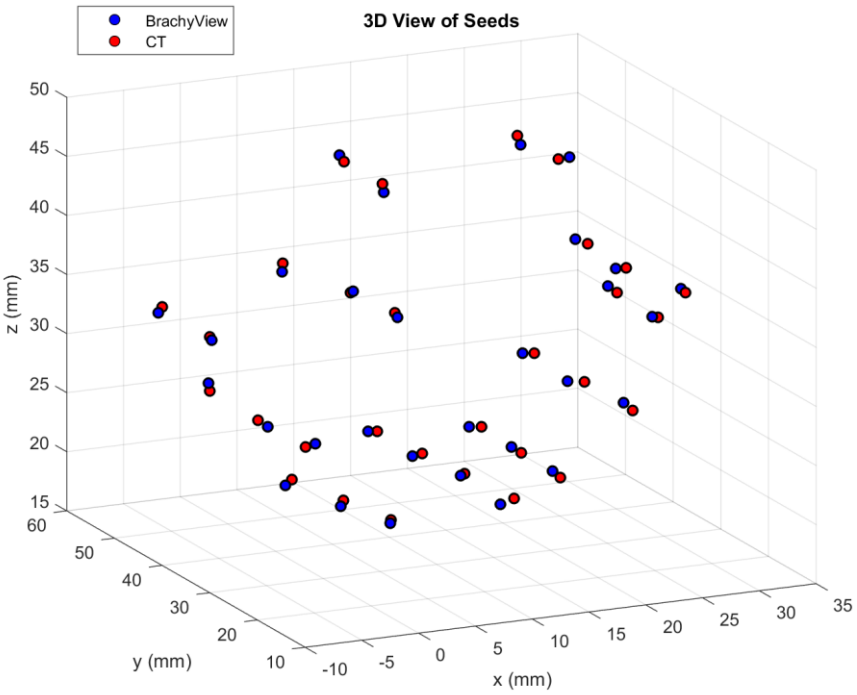

Fig. 5.7: 3D scatter plot of reconstructed seeds from BrachyView and CT determined seed positions.

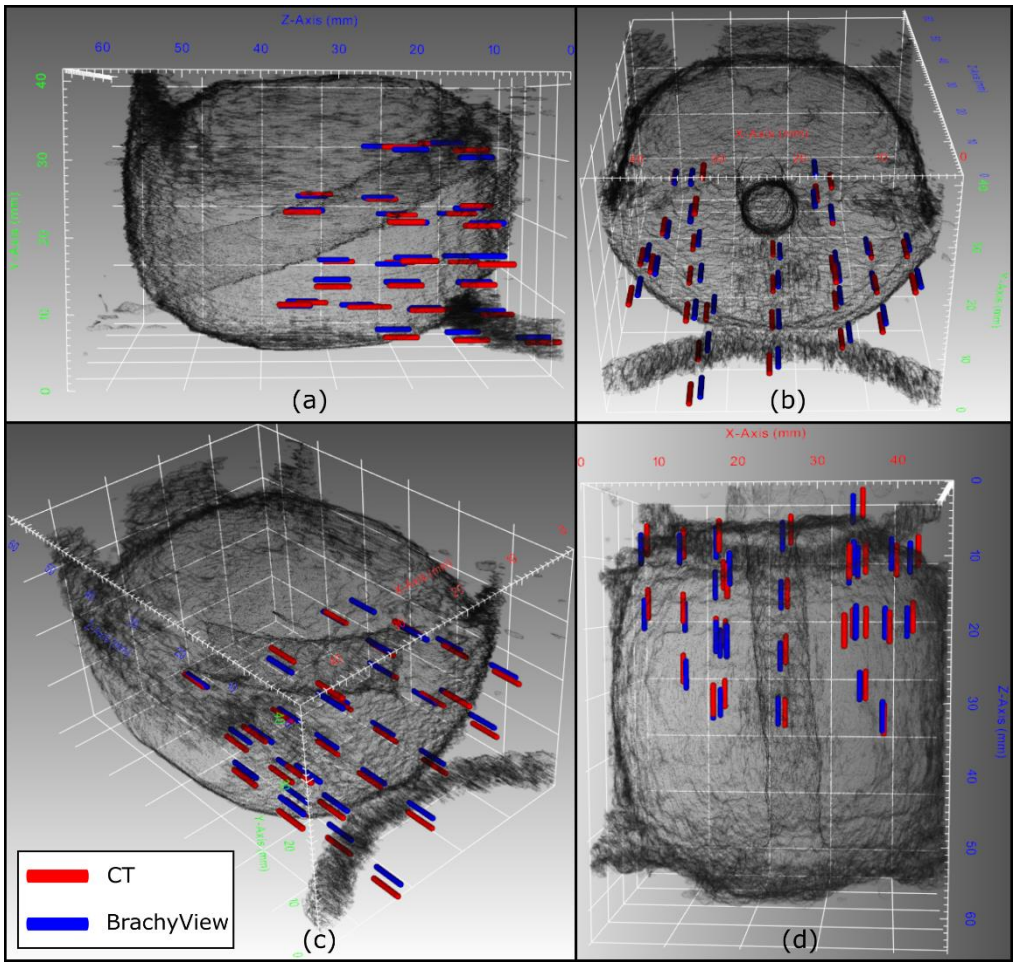

Figure 5.8: Screen shot of software interface depicting 3D prostate model reconstructed from US images with reconstructed seed positions from both the BrachyView and CT data set co-registered into a single coordinate system.

Chapter Six: Discussion

PMMA Phantom Experiment

Despite the use of a single detector and a stepper motor to mimic the presence of three devices, the BrachyView system is able to reconstruct seed positions using the triangulation method. In the 20 seeds experiment, the seeds were found within the PMMA phantom with an accuracy of 1-2mm as compared with the CT scan within a distance of 6cm from the collimator. The multi-seed plan imitated a more clinically relevant case in respect to the feasibility study performed by Petasecca et al., to demonstrate the capabilities of BrachyView in resolving multiple seeds in real time with sub-millimeter accuracy. Although the setup is still short of a full clinical LDR brachytherapy plan (between 60-120 seeds), the superior resolution of the BrachyView will allow localisation of the most distal seeds from the pinhole (50-60mm).

In this experiment a single detector was translated via a stepper motor to mimic a triple chip setup. This introduces a systematic error in determining the position of the pinhole which is used to localise the seeds in the phantom, therefore sabotaging the overall accuracy of the reconstruction. A fully functional multiple chip assembly will allow for a rigid coordinate system and remove uncertainties introduced by a moving detector. This will also obviate the need for complicated alignment methods, which will further reduce uncertainties in the system.

BrachyView is aimed to be used during the implantation procedure, as an intraoperative imaging modality, whereby seeds can be imaged during the treatment before they have been dropped by the needle. This will allow for online monitoring of the dose distribution and thus active corrections on the location of the seeds with in the prostate volume. The BrachyView system is not capable of performing day 30 post-implant dosimetry, as the seed activity would be considerably reduced, and resolving the seeds would be impossible due to poor signal to background ratio.

A background subtraction method was developed to account for accumulative background counts which would otherwise saturate the signal. Using this algorithm, it was hypothesized that background subtraction would be necessary after 30 implanted seeds, as the signal to background ratio will become significantly poor. The subtraction method will require an iterative needle implantation procedure and thus cannot be implemented in a post-implant dosimetry, as resolving all the implanted seeds would prove very difficult. Although beyond the scope of this experiment, this simple methodology demonstrates the capabilities of the BrachyView to localise sources in a full-size clinical implant. The flat lead collimator is responsible for the current signal to background ratio, this problem is addressed with a cylindrical tungsten collimator which allows for better lateral shielding from the phantom or the patient.

Dose calculation using TG-43 have shown the importance of seed accuracy and the outcomes of dose variations due to seed misplacement. The isodose plots show variations due in dose distributions between the BrachyView and CT dataset. The largest discrepancies are at the slices where seed position variations are high between the two data sets. The dose histogram showed 8.61% deviation between the BrachyView and CT datasets, despite seed position discrepancies of 1-2mm.

The Air KERMA strength of the seeds was measured by a well chamber at the St. George hospital. This procedure was performed post implantation, and ensured a uniform dose delivery to the phantom. The measured values ranged from 0.426 – 0.481 $\mu Gy\ m^2 h^{-1}$. The activity of each individual seed was used to calculate the overall dose distribution.
In this experiment, a rigid PMMA phantom was used for seed implantation, and thus the co-registration of the two data sets was rigid and quite simple. A point to point co-registration is sufficient for the purposes of this study. However, in clinical conditions Ultrasound images are acquired in the lithotomy position via a rectal probe and the CT images are taken with the patient laid down on the CT couch. To allow for a rigid reconstruction in a clinical setting, a mechanical co-registration is under investigation, one which features the TRUS probe and BrachyView on opposite halves of the stepper unit and thus sharing a coordinate system. Another proposed method is the use of fiducial markers that can be picked up by the ultrasound images that will guide the co-registration.

Gel Phantom Experiment

The new improved BrachyView probe features a triple chip Timepix detector enclosed in a cylindrical tungsten collimator. In this experiment 30 active seeds were implanted in a gel prostate phantom following a realistic implantation process. BrachyView was used in conjunction with a TRUS probe to localise the implanted seeds with respect to the anatomical features resolved by the ultrasound images. CT images of the whole setup were acquired for a set standard. The BrachyView probe was able to successfully reconstruct the locations of all 30 implanted seeds. A maximum discrepancy of 1.78mm was observed between the BrachyView and CT determined seed positions. It was determined that 75% of the BrachyView resolved seeds lay within 1mm of the CT determined positions. Each component of the discrepancies between CT and BrachyView was examined, with Z direction discrepancies all within the submillimeter range, the X direction discrepancies showed 68% within 1mm and the largest differences were found in the Y direction. The sources of error in the reconstruction are determined to be the calculated position of the pinholes relative to the origin (corner of the first Timepix chip), and the ability to accurately locate the COM of the seeds. An error of 0.1mm in the position of the pinhole will result in an uncertainty of ± 0.56mm in the X or Y direction, this effect is smaller in the Z direction ± 0.27mm. This calculation is based on a model determined in the previous study conducted by Petasecca et. al.
The CT determined seed locations were found by defining the centre of the each seed from the CT slices. The slice width used to image the seeds was 1mm which limits the accuracy of determining the centre of the seeds particularly in the Y direction (along their length).

The physical compression of the gel phantom was observed by the insertion of the probes, which contributes to the movement of the already implanted seeds. The non-rigid phantom changes shape in the process of inserting and removing the BrachyView and the TRUS probes, this is most relevant in the Y direction. This replicates a clinical scenario where the soft tissue of the internal organs is compressed due to the implantation of the needles, even without removing the TRUS probe. This problem can be addressed by inserting a thin plastic shell, into which the probes can slide in and out without deforming the internal organs.
By stacking the ultrasound slices of the prostate, the volume of the gel phantom was successfully reconstructed. The internal features of prostate, the urethra and seminal

vesicles, and the outline of the organ were clearly visible in the visualisation software. The rigid transformation of the BrachyView and CT coordinate systems into the TRUS coordinate system was successfully achieved. The 30 implanted seeds were located within the prostate volume of the gel phantom.

BrachyView is a powerful tool for Quality Check which allows the localisation of Permanent Brachytherapy seeds implanted within the prostate. It requires no extra time for image acquisition and is performed within the operating room thus the patient does not need to be moved. A day 0 post-implant CT is not required and thus no additional dose is delivered to the patient and the uncertainties that arise with the use of CT can be avoided.

References

[1] Bill-Axelson, A, Holmberg, L, Ruutu, M, Garmo, H, Stark, JR, Busch, C, Nordling, S, Häggman, M, Andersson, S, Bratell, S, Spängberg, A, Palmgren, J, Steineck, G, Adami, H, & Johansson, J (2011), '**Radical Prostatectomy versus Watchful Waiting in Early Prostate Cancer**', New England Journal of Medicine, vol. 364, no. 18, p. 1708. Available from: 10.1056/NEJMoa1011967. [30 May 2017].

[2] Boladeras, A., Santorsa, L., Gutierrez, C., Martinez, E., Pera, J., Pino, F., Suarez, J., Ferrer, F., Díaz, A., Polo, A. and Guedea, F. (2014). **External beam radiotherapy plus single-fraction high dose rate brachytherapy in the treatment of locally advanced prostate cancer**. *Radiotherapy and Oncology*, 112(2), pp.227-232.

[3] Peeters, S., Heemsbergen, W., Koper, P., van Putten, W., Slot, A., Dielwart, M., Bonfrer, J., Incrocci, L. and Lebesque, J. (2006). **Dose-Response in Radiotherapy for Localized Prostate Cancer: Results of the Dutch Multicenter Randomized Phase III Trial Comparing 68 Gy of Radiotherapy With 78 Gy**. *Journal of Clinical Oncology*, 24(13), pp.1990-1996.

[4] Zelefsky, M., Fuks, Z., Happersett, L., Lee, H., Ling, C., Burman, C., Hunt, M., Wolfe, T., Venkatraman, E., Jackson, A., Skwarchuk, M. and Leibel, S. (2000). **Clinical experience with intensity modulated radiation therapy (IMRT) in prostate cancer**. *Radiotherapy and Oncology*, 55(3), pp.241-249.

[5] Zietman, AL 2002, '**Localized prostate cancer: brachytherapy**', Current Treatment Options In Oncology, vol. 3, no. 5, pp. 429-436.

[6] Zaorsky, NG, Doyle, LA, Yamoah, K, Andrel, JA, Trabulsi, EJ, Hurwitz, MD, Dicker, AP, & Den, RB 2014, '**High dose rate brachytherapy boost for prostate cancer: a systematic review**', Cancer Treatment Reviews, vol. 40, no. 3, pp. 414-425. Available from: 10.1016/j.ctrv.2013.10.006. [30 May 2017].

[7] Trinh, Q., Bjartell, A., Freedland, S., Hollenbeck, B., Hu, J., Shariat, S., Sun, M. and Vickers, A. (2013). **A Systematic Review of the Volume–Outcome Relationship for Radical Prostatectomy**. *European Urology*, 64(5), pp.786-798. [25 May 2017].

[8] Hegemann, N., Guckenberger, M., Belka, C., Ganswindt, U., Manapov, F. and Li, M. (2014). **Hypofractionated radiotherapy for prostate cancer. Radiation Oncology**, 9(1). [20 April 2017].

[9] Voulgaris, S., Nobes, J., Laing, R. and Langley, S. (2008). **State-of-the-art: prostate LDR brachytherapy**. Prostate Cancer and Prostatic Diseases, 11(3), pp.237-240. [25 April 2017].

[10] Pfeiffer, D., Sutlief, S., Feng, W., Pierce, H. and Kofler, J. (2008). **AAPM Task Group 128: Quality assurance tests for prostate brachytherapy ultrasound systems**. *Medical Physics*, 35(12), pp.5471-5489. [25 April 2017].

[11] Henry, A., Rodda, S., Mason, M., Musunuru, H., Al-Qaisieh, B., Bownes, P., Smith, J., Franks, K., Carey, B. and Bottomley, D. (2015). **The Effect of Dose and Quality Assurance in Early Prostate Cancer Treated with Low Dose Rate Brachytherapy as Monotherapy**. *Clinical Oncology*, 27(7), pp.382-386. [30 May 2017].

[12] Solhjem, M., Davis, B., Pisansky, T., Wilson, T., Mynderse, L., Herman, M., King, B. and Geyer, S. (2004). **Prostate volume measurement by transrectal ultrasound and computed tomography before and after permanent prostate brachytherapy**. *International Journal of Radiation Oncology*Biology*Physics*, 60(3), pp.767-776. [30 May 2017].

[13] Daanen, V., Gastaldo, J., Giraud, J., Fourneret, P., Descotes, J., Bolla, M., Collomb, D. and Troccaz, J. (2006). **MRI/TRUS data fusion for brachytherapy.** *The International Journal of Medical Robotics and Computer Assisted Surgery*, 2(3), pp.256-261. 30 May 2017].

[14] Shaikh, T., Zaorsky, N., Ruth, K., Chen, D., Greenberg, R., Li, J., Crawford, K. and Horwitz, E. (2015). **Is it necessary to perform week three dosimetric analysis in low-dose-rate brachytherapy for prostate cancer when day 0 dosimetry is done? A quality assurance assessment**. *Brachytherapy*, 14(3), pp.316-321. [30 May 2017].

[15] Takiar, V., Pugh, T., Swanson, D., Kudchadker, R., Bruno, T., McAvoy, S., Mahmood, U. and Frank, S. (2014). **MRI-based sector analysis enhances prostate palladium-103 brachytherapy quality assurance in a phase II prospective trial of men with intermediate-risk localized prostate cancer**. *Brachytherapy*, 13(1), pp.68-74. [30 May 2017].

[16] Ravi, A, Caldwell, C, Keller, B, Reznik, A, & Pignol, J 2007, '**Online gamma-camera imaging of 103Pd seeds (OGIPS) for permanent breast seed implantation**', Physics in Medicine and Biology, vol. 52, no. 19, pp. 5921-5932. Available from: 10.1088/0031-9155/52/19/013. [30 May 2017].

[17] Han, Z., Safavi-Naeini, M., Alnaghy, S., Cutajar, D., Guatelli, S., Petasecca, M., Franklin, D., Malaroda, A., Carrara, M., Bucci, J., Zaider, M., Lerch, M. and Rosenfeld, A. (2014). **Radiation dose enhancement at tissue-tungsten interfaces in HDR brachytherapy**. *Physics in Medicine and Biology*, 59(21), pp.6659-6659. [5 May 2017]

[18] Petasecca, M., Loo, K., Safavi-Naeini, M., Han, Z., Metcalfe, P., Meikle, S., Pospisil, S., Jakubek, J., Bucci, J., Zaider, M., Lerch, M., Qi, Y. and Rosenfeld, A. (2013). **BrachyView: Proof-of-principle of a novel in-body gamma camera for low dose-rate prostate brachytherapy**. *Medical Physics*, 40(4), p.041709. [30 May 2017].

[19] Jakůbek, J. (2009). **Semiconductor Pixel detectors and their applications in life sciences**. *Journal of Instrumentation*, 4(03), pp.P03013-P03013. [30 May 2017].

[20] Campbell, M. (2011). **10 years of the Medipix2 Collaboration**. *Nuclear Instruments and Methods in Physics Research Section A: Accelerators, Spectrometers, Detectors and Associated Equipment*, 633, pp.S1-S10. [30 May 2017].

[21] Jakubek, J. (2009). **Energy-sensitive X-ray radiography and charge sharing effect in pixelated detector**. *Nuclear Instruments and Methods in Physics Research Section A: Accelerators, Spectrometers, Detectors and Associated Equipment*, 607(1), pp.192-195. [20 May 2017].

[22] Bisogni, M., Cirrone, G., Cuttone, G., Del Guerra, A., Lojacono, P., Piliero, M., Romano, F., Rosso, V., Sipala, V. and Stefanini, A. (2009). **Medipix2 as a tool for proton beam characterization**. *Nuclear Instruments and Methods in Physics Research Section A: Accelerators, Spectrometers, Detectors and Associated Equipment*, 607(1), pp.48-50. [30 May 2017].

[23] Michel, T., Bohnel, M., Durst, J., Sievers, P. and Anton, G. (2009). **Low Energy Dosimetry With Photon Counting Pixel Detectors Such as Medipix**. *IEEE Transactions on Nuclear Science*, 56(2), pp.417-423. [30 May 2017].

[24] Weaver, M., Petasecca, M., Lerch, M., Cutajar, D., Jakůbek, J., Pospíšil, S. and Rosenfeld, A. (2011). **Dosimetry verification in eye brachytherapy using silicon pixelated detectors.** *Radiation Measurements*, 46(12), pp.2010-2013. [30 May 2017].

[25] Alnaghy, S., Safavi-Naeini, M., Franklin, D., Han, Z., Cutajar, D., Petasecca, M., Lerch, M. and Rosenfeld, A. (2016). **Analytical Modelling and Simulation of Single and Double Cone Pinholes for Real-Time In-Body Tracking of an HDR Brachytherapy Source**. *IEEE Transactions on Nuclear Science*, 63(3), pp.1375-1385. [30 May 2017].

[26] Stock, R. (2002). **Importance of Post-Implant Dosimetry in Permanent Prostate Brachytherapy**. European Urology, 41(4), pp.434-439.

[27] Wang, G., Kalra, M., Murugan, V., Xi, Y., Gjesteby, L., Getzin, M., Yang, Q., Cong, W. and Vannier, M. (2015). **Vision 20/20: Simultaneous CT-MRI - Next chapter of multimodality imaging**. Medical Physics, 42(10), pp.5879-5889.

[28] Loo, K., Jakubek, J., Zemlicka, J., Petasecca, M., Safavi-Naeini, M., Bucci, J., Zaider, M. and Rosenfeld, A. (2014). **BrachyView: Feasibility study into the application of Timepix detectors for soft tissue thickness imaging in prostate brachytherapy treatment**. Radiation Measurements, 71, pp.329-332.

[29] Alnaghy, S., Loo, K., Cutajar, D., Jalayer, M., Tenconi, C., Favoino, M., Rietti, R., Tartaglia, M., Carriero, F., Safavi-Naeini, M., Bucci, J., Jakubek, J., Pospisil, S., Zaider, M., Lerch, M., Rosenfeld, A. and Petasecca, M. (2016). **BrachyView: multiple seed position reconstruction and comparison with CT post-implant dosimetry**. Journal of Instrumentation, 11(05), pp.P05002-P05002.

[30] Alnaghy, S., Cutajar, D., Bucci, J., Enari, K., Safavi-Naeini, M., Favoino, M., Tartaglia, M., Carriero, F., Jakubek, J., Pospisil, S., Lerch, M., Rosenfeld, A. and Petasecca, M. (2017). **BrachyView: Combining LDR seed positions with transrectal ultrasound imaging in a prostate gel phantom**. *Physica Medica*, 34, pp.55-64.